



# TextPecker: Rewarding Structural Anomaly Quantification for Enhancing Visual Text Rendering

Hanshen Zhu<sup>1,\*</sup>, Yuliang Liu<sup>1</sup>, Xuecheng Wu<sup>2</sup>, An-Lan Wang<sup>2</sup>, Hao Feng<sup>2</sup>, Dingkang Yang<sup>2</sup>, Chao Feng<sup>2</sup>, Can Huang<sup>2</sup>, Jingqun Tang<sup>2,†</sup>, Xiang Bai<sup>1,✉</sup>

<sup>1</sup>Huazhong University of Science and Technology <sup>2</sup>ByteDance  
 {zhs, ylliu, xbai}@hust.edu.cn, jingquntang@bytedance.com

<https://github.com/CIaweiy/TextPecker>

## Abstract

Visual Text Rendering (VTR) remains a critical challenge in text-to-image generation, where even advanced models frequently produce text with structural anomalies such as distortion, blurriness, and misalignment. However, we find that leading MLLMs and specialist OCR models largely fail to perceive these structural anomalies, creating a critical bottleneck for both VTR evaluation and RL-based optimization. As a result, even state-of-the-art generators (e.g., SeedDream4.0, Qwen-Image) still struggle to render structurally faithful text. To address this, we propose **TextPecker**, a plug-and-play structural anomaly perceptive RL strategy that mitigates noisy reward signals and works with any text-to-image generator. To enable this capability, we construct a recognition dataset with character-level structural-anomaly annotations and develop a stroke-editing synthesis engine to expand structural-error coverage. Experiments show that TextPecker consistently improves diverse text-to-image models; even on the well-optimized Qwen-Image, it significantly yields average gains of 4% in structural fidelity and 8.7% in semantic alignment for Chinese text rendering, establishing a new state-of-the-art in high-fidelity VTR. Our work fills a gap in VTR optimization, providing a foundational step towards reliable and structural faithful visual text generation.

## 1. Introduction

Text-to-image generation has witnessed remarkable progress in producing photorealistic and detail-rich results [2, 10, 41, 44]. With these advancements, Visual Text Rendering (VTR), the task of generating legible and semantically consistent text within images, has emerged as a challenging and evolving frontier [3, 55, 65]. However, the recent surge

\*Part of this work was done during Hanshen Zhu’s internship at ByteDance. †Project leader. ✉Corresponding author.

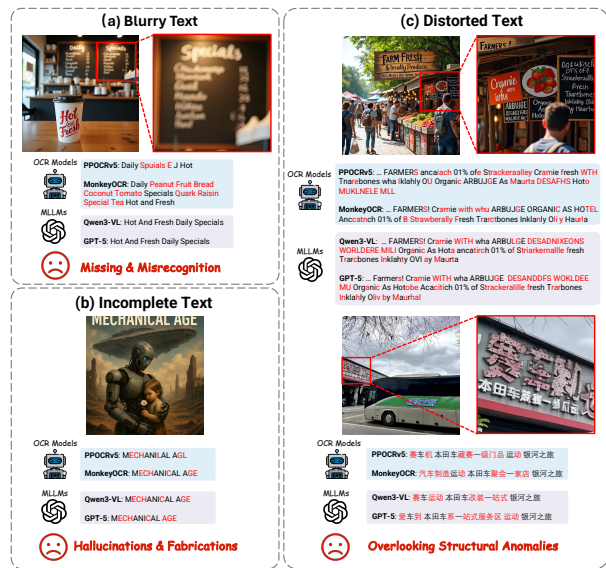


Figure 1. Existing OCR models and MLLMs struggle to perceive fine-grained structural anomalies in rendered text images, creating a key bottleneck for both VTR evaluation and RL-based optimization. Misrecognized characters are highlighted in RED.

of specialized image generators (e.g., Flux-series [28]) and unified generative models (e.g., GPT-4o [39], BAGEL [12]) still struggle with VTR tasks, producing visual text with distortion, blurriness, misalignment, or missing characters [65]. Prior works [9, 18, 20, 55] mitigate these issues with reinforcement learning (RL): the generated text is first recognized through OCR models [15, 53] or Multimodal Large Language Models (MLLMs) [1, 60, 69], then rule-based scores (e.g., edit distance to the prompt) are computed and used as rewards. To evaluate text rendering performance, existing metrics [6, 14, 20] follow an analogous paradigm. This prevailing paradigm, however, rests on a flawed premise.

We identify a critical **bottleneck** shared by both VTR evaluation and reinforcement learning process: **a lack of fine-grained structural anomaly perception in rendered**

**text.** As illustrated in Fig. 1, OCR models [15, 53] and MLLMs [1, 40] are inherently ill-suited for this task. Their failures manifest in two primary ways: (1) **Misinterpretation:** They over-rely on linguistic priors to “correct” or hallucinate semantic content from structurally flawed text, thereby ignoring subtle glyph-level defects (*e.g.*, stroke deletions, misalignments, or spurious attachments). (2) **Invisibility:** They often fail to detect or simply dismiss low-confidence text regions, such as those with significant blurriness or distortion, treating them as non-existent. Therefore, evaluators yield unreliable text-accuracy estimates and fail to assess structural quality, and reward signals become misleading. As a direct result, even state-of-the-art generators (*e.g.*, Qwen-Image [55], SeedDream4.0 [3]) still struggle to render structurally faithful text. Our quantitative analysis in Tab. 2 further substantiates this issue.

Building on these insights, we propose **TextPecker**, a plug-and-play structural anomaly perceptive RL strategy for visual text rendering. At its core, TextPecker replaces noisy OCR-based rewards with a perception-guided composite reward that jointly captures semantic alignment and structural fidelity. Its structural term is sensitive to fine-grained glyph deformation and distortion, assigning reliable penalties to subtle defects that deceive structure-blind OCR and destabilize policy learning. This yields stable credit assignment and seamlessly integrates into any text-to-image generator without architectural changes. To construct this reward, we address the scarcity of fine-grained structural annotations by building a hybrid dataset that couples two complementary sources: (1) images with authentic generative artifacts from various text-to-image models, meticulously annotated at the character-level, and (2) synthetic data from our stroke-editing engine, crafted to expand error diversity while including normal characters for robust recognition.

Extensive experimental results demonstrate that our introduced TextPecker delivers consistent and significant improvements across diverse generators, including FLUX [28], SD3.5 [16], and Qwen-Image [55]. Remarkably, For FLUX, our method yields dramatic gains over its base version (*e.g.* +38.3% Sem. and +31.6% Qua.) while also substantially outperforming the OCR-reward baseline. This advancement becomes even more pronounced on the highly-optimized Qwen-Image. In the challenging domain of Chinese text rendering, our approach achieves gains of 8.7% in semantic alignment and 4% in structural fidelity, establishing a new state-of-the-art in high-fidelity VTR.

We summarize our **contributions** as follows:

- We identify a critical **bottleneck** in VTR: the lack of fine-grained structural perception in current OCR-based evaluators, which hinders effective VTR optimization.
- We propose **TextPecker**, a plug-and-play structural anomaly perceptive RL strategy that seamlessly integrates into any text-to-image generators.
- We construct a large-scale dataset with character-level structural anomaly annotations, addressing the data scarcity and enabling fine-grained structural perception for reward modeling.
- Our method consistently improves leading generators and sets a new state-of-the-art in VTR, with notable gains even on the highly optimized Qwen-Image.

## 2. Related Work

### 2.1. Visual Text Rendering

Text images are unique and crucial information media in modern digital society. Mainstream text rendering methods broadly fall into two categories. The first focuses on specialized modules to incorporate additional constraints, such as glyph information [38, 48, 61, 64] for text morphology control, or layout guidelines [7, 19, 52, 63] for precise text placement. The second focuses on improving text encoder designs. A prevailing explanation for the text rendering’s difficulty is that the text information often degrades or is inadequately preserved during encoding. To mitigate this, subsequent works [8, 36, 67] introduce special tokens for the rendered text or adopt tokenizer-free encoders like ByT5 [59]. With recent advances in generative models, specialized generators [3, 16, 28, 55] and unified generative models [12, 32, 56] already exhibit substantial text rendering capabilities without relying on ad-hoc designs such as glyph conditions. Despite these improvements, they still struggle with text rendering tasks, producing visual text with distortion, blurriness, misalignment, or missing characters [65].

### 2.2. Evaluations for VTR

The assessment of VTR has predominantly centered on textual accuracy [6, 14, 20, 49]. A key challenge, particularly in non-glyph-conditioned generation, is the potential order mismatch between generated and target text. To address this, Lex-Art[66] proposed Pairwise Normalized Edit Distance (PNED), which combines Hungarian matching [26, 37] with a penalty for unmatched words. TIF-Bench added global normalization to yield GNED[54], reducing sensitivity to text-length imbalance. Fang et al. [17] directly use Qwen2.5-VL [1] as end-to-end VTR evaluators, yet it suffers from hallucination and inaccuracies. Notably, recent works have also recognized the importance of structural quality of text. Font-Agent [29] presents a stroke-aware font quality assessor, yet it is limited to single-character evaluations. He et al. [24] addresses OCR hallucinations in degraded documents, but is confined to document analysis domain.

Reward models are crucial for aligning generative models with human preferences during post-training optimization. Numerous efforts have largely improved reward models for general visual quality assessment [51, 57, 58]. Unlike subjective protocols such as aesthetic or quality, existing VTR

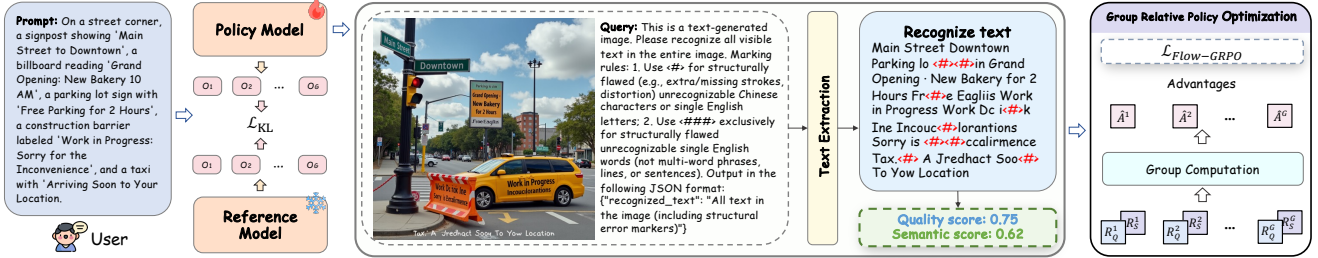


Figure 2. **Schematic illustration of the TextPecker framework.** Given a generative prompt, we first sample  $G$  candidate outputs  $\{o_i\}_{i=1}^G$  from the reference policy model  $\pi_{\theta_{\text{ref}}}$ . Each  $o_i$  is sent to a structure-aware recognizer to extract fine-grained generated text, with markers indicating structurally anomalous text. We then compute the joint reward  $\mathcal{R}_i$ , comprising a weighted sum of semantic alignment and structural quality scores (Sec. 3.2.1). Each  $\mathcal{R}_i$  is normalized to a group relative advantage  $A_i$ . Finally, we optimize the current policy model  $\pi_{\theta}$  by maximizing  $A_i$  while enforcing proximity to  $\pi_{\text{ref}}$  via KL divergence.

reward modeling [9, 18, 20, 21] has primarily focused on textual accuracy, which is typically assessed by *de facto* evaluators such as standard OCR models [15, 53] or MLLMs like Qwen2.5-VL [1].

However, these methods for both evaluation and reward modeling are fundamentally constrained by their inability to perceive fine-grained structural anomalies, leading to unreliable accuracy estimates and misleading rewards. In response, TextPecker’s fine-grained, perception-guided composite reward moves beyond the noisy signals of OCR-based methods, enabling the joint quantification of semantic accuracy and structural fidelity.

## 3. Methodology

### 3.1. Preliminaries

Reinforcement learning (RL) is a common and effective paradigm for improving text rendering in text-to-image models [3, 28, 55], with widely adopted variants such as DPO [42] and GRPO [22]. We focus on GRPO, a critic-free on-policy method that stabilizes policy optimization via group-wise relative advantages and intra-group reward normalization. However, due to the deterministic nature of flow-matching [33, 35] models, they are not intrinsically designed for reinforcement learning. Flow-GRPO [34] extends GRPO to the rectified-flow setting by injecting stochasticity into the integration process. Specifically, it converts the deterministic dynamics into a stochastic differential equation:

$$dx_t = \left( v_t + \frac{\sigma_t^2}{2t} (x_t + (1-t)v_t) \right) dt + \sigma_t dw_t, \quad (1)$$

where  $v_t = v_{\theta}(x_t, t, c)$  is the network-predicted velocity,  $dw_t$  denotes Brownian motion, and  $\sigma_t = a\sqrt{\frac{t}{1-t}}$  controls the magnitude of stochasticity.

For VTR Optimization, prior works [9, 18, 20, 34] predominantly leverage a string-level accuracy reward:  $S = 1 - N_e/N_t$ , where  $N_t$  denotes the length of target string and

$N_e$  is the edit distance between the target string and the OCR-extracted content. As discussed earlier (cf. Fig. 1), existing OCR Models [15, 53] and MLLMs [1] prioritize semantic recovery over glyph integrity, hallucinating corrections for structurally flawed text and omitting low-confidence distorted regions. Such behaviors depress the edit distance  $N_e$  and inflate the reward score  $S$ , resulting in biased rewards that hinder effective optimization.

### 3.2. TextPecker

As shown in Fig. 2, we introduce **TextPecker**, a plug-and-play RL strategy for enhancing VTR with fine-grained structural perception. Unlike conventional methods that rely on noisy OCR signals and overlook structural flaws, TextPecker redefines reward modeling by jointly optimizing semantic alignment and structural fidelity. Integrating this perception-guided composite reward into the RL loop yields consistent gains across diverse generators.

#### 3.2.1. Structure-aware Reward Functions

To address the structural blindness and overconfident scoring of prior OCR-based methods, our reward formulation is built upon a **structure-aware assessment module**. As illustrated in Fig. 2, this module identifies fine-grained structural anomalies in the generated text (*e.g.*, missing or spurious strokes) and flags them with special markers. The detailed construction of this module is presented in Sec. 3.2.2. Assuming we have such a module, we formulate our composite reward as follows.

**Structural Quality Score ( $S_Q$ ).** An intuitive way to quantify structural quality is to measure the proportion of “bad” characters. We define the structural quality score,  $S_Q$ , based on the ratio of structurally anomalous characters to the total number of characters. However, for powerful generators, structural errors are often rare but visually jarring when they do occur. To amplify the penalty for such infrequent yet critical failures, we introduce a scaling factor  $\omega > 1$ . The

final score is thus formulated as:

$$S_Q = \text{clip}\left(1 - \omega \frac{N_a}{N_P}, 0, 1\right), \quad (2)$$

where  $N_P$  is the total number of characters in the generated text  $\mathcal{P}$ , and  $N_a$  is the number of characters flagged as anomalous by our assessor. Here,  $\text{clip}$  constrains the value to the range  $[0, 1]$ .

**Semantic Alignment Score ( $S_E$ ).** Unlike prior OCR-based rewards that treat text as a simple long string, we argue that word-level matching is crucial for accurately assessing text that may not be rendered in the same order as the prompt. Inspired by [54, 66], we also find it necessary to penalize any unmatched words, which typically include extraneous or repeated texts in the generated output, as well as missing textual content from the target prompt. Therefore, we formulate our semantic alignment score as:

$$S_E = 1 - \frac{\sum_{(t_i, p_j) \in \mathcal{M}} \text{NED}(t_i, p_j) + \text{Penalty}(\mathcal{T}, \mathcal{P}, \mathcal{M})}{\max(|\mathcal{T}|, |\mathcal{P}|)}. \quad (3)$$

Here,  $\mathcal{T}$  and  $\mathcal{P}$  are the sets of words in the target and generated text, respectively.  $\mathcal{M}$  represents the optimal word pairing between  $\mathcal{T}$  and  $\mathcal{P}$ , found via the Hungarian algorithm to achieve the minimum alignment cost based on Normalized Edit Distance (NED). The  $\text{Penalty}(\cdot)$  term is the count of any unmatched words. This ensures that both superfluous generated words and missing target words contribute to the overall error. The final score  $S_E$  is also clipped to the range of  $[0, 1]$ , where a higher value indicates better semantic alignment.

**Composite Reward ( $\mathcal{R}$ ).** Finally, we formulate the overall TextPecker reward  $\mathcal{R}$  as a weighted sum of the two scores, allowing for a joint optimization of both aspects:

$$\mathcal{R} = w_E S_E + w_Q S_Q, \quad w_E + w_Q = 1. \quad (4)$$

### 3.2.2. Structural Perceptive Data Construction

Our structure-aware reward relies on a robust assessor for fine-grained structural anomalies, but the requisite labeled data is critically scarce. To construct a large-scale, high-quality dataset, we proceed in **three steps** (Fig. 3):

**Step 1: Text-rich Image Generation.** The initial step involves constructing a large-scale dataset of text-rich visual images, covering diverse structural error types. Specifically, for English text generation, we draw prompts from TextAtlas5M [49] and Lex-10k [66], and leverage multiple English-capable generative models (Anytext, Stable Diffusion v1-5 [43], Stable Diffusion 3.5 [16], Flux [28], SeedDream3.0 [18], Qwen-Image [55]) to generate such images. For Chinese text generation, we first sample a comprehensive text

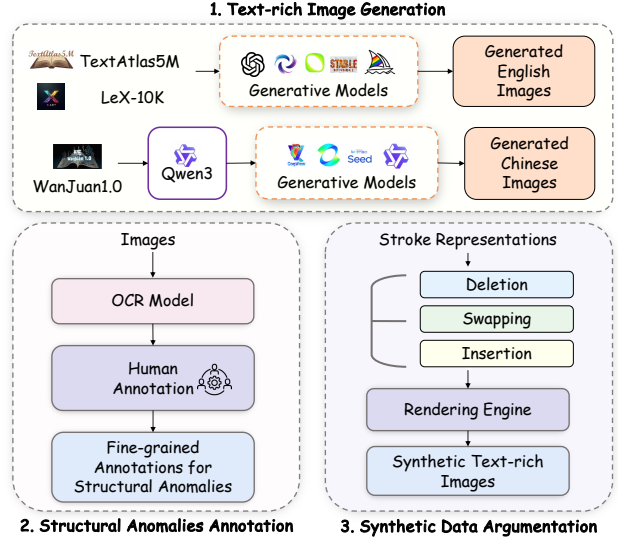


Figure 3. The illustration of proposed data construction pipeline.

corpus from WanJuan1.0 [23], ensuring coverage of modern Chinese common characters. We then use Qwen3-235B-A22B [60] to generate descriptions of various font styles, which are integrated with the corpus to form final prompts for models including Cogview4 [13], Kolors [27], SeedDream3.0 [18], and Qwen-Image [55].

**Step 2: Structural Anomaly Annotation.** Generated text-rich images exhibit diverse structural anomalies. We define such anomalies as any structural distortion impairing semantic recognition, caused by blurring, warping, missing strokes, or redundant artifacts. To streamline annotation, we first leverage OCR models [15] to obtain preliminary recognition results. Annotators then identify and rectify fine-grained character-level structural flaws with a **special marker** (as illustrated in Fig. 2). For words with severe structural adhesion that prevents accurate character counting, we use a distinct placeholder, yielding a dataset with refined fine-grained labels for structural anomalies.

**Step 3: Synthetic Data Augmentation.** While Step 2’s annotations capture common structural anomalies, models trained solely on them exhibit two key limitations: poor generalization to unseen anomalies and degraded recognition of Chinese characters (Tab. 4). This stems from the intrinsic complexity of Chinese: unlike the linear morphology of English, Chinese characters have a 2D spatial composition and a vast inventory of over 8,000, causing a combinatorial explosion of structural anomalies beyond what exhaustive annotation can cover. To overcome this, we introduce a synthesis-based augmentation that programmatically generates diverse erroneous and canonical Chinese characters.

We start by representing Chinese characters as compositions of fundamental strokes, modeled as ordered sequences using stroke order data from public resources. To streamline manipulation, we uniformly sample points along each stroke

Table 1. Statistics of our constructed text-rich image recognition dataset with structural-anomaly labels at box and image levels. Proportions are computed over all instances.

Data Type	Level	Samples	Proportion
Manual Annotations	Box	559.6K	39.32%
	Image	131.1K	9.21%
Synthetic Anomaly Text	Box	452.5K	31.80%
	Image	100.0K	7.03%
Synthetic Normal Text	Box	150.0K	10.54%
	Image	30.0K	2.10%
<b>Total</b>	-	1.4M	100%

to enable manipulation. With stroke sequences and their point representations, we define three stroke-level structural edit operators. We apply them sequentially and compose them to produce diverse structural anomalies. (1) *Stroke Deletion*: removes a controlled subset of strokes. (2) *Stroke Swapping*: exchanges the locations of disjoint stroke pairs by aligning centroids. (3) *Stroke Insertion*: adds strokes sampled from other characters. These operators generate structurally anomalous characters, we then build a rendering engine on top of SynthTIGER [62] and use it to place structurally anomalous and canonical text onto diverse backgrounds and layouts, producing text-rich images. We merge the annotated and synthetic data to form the final training and test splits, with dataset statistics and visualized distributions shown in Tab. 1.

## 4. Experiments

### 4.1. Experimental settings

Additional implementation details of our method, Baselines, dataset, and metrics are provided in the Appendix.

**Implementation Details.** We adopt Qwen3-VL-8B [60] and InternVL3-8B [69] as the base architecture for TextPecker, leveraging their strong general recognition performance, robust cross-modal alignment, and native support for boundary box input. Fully supervised fine-tuning uses a batch size of 2, gradient accumulation steps of 32, learning rate of 5e-6, warm-up ratio of 0.05, and runs for 2 epochs. For VTR optimization, we employ Flow-GRPO [34] and validate on three popular models: SD3.5-M [16], Flux.1[dev] [28], and Qwen-Image [55]. We set  $\omega = 5$  and  $w_E = w_Q = 0.5$  and adopt the Qwen3-VL-based variant for reward function. Following Flow-GRPO [34], other hyperparameters vary across models but are consistent within each; full details are provided in the Appendix. Both the recognizer training and VTR optimization experiments are conducted on 32 NVIDIA H20 GPUs.

**Metrics and Datasets.** We design two tasks, Text Structural Anomaly Perception (*TSAP*) and Canonical Text Recognition (*CTR*), to evaluate models’ fine-grained recognition abil-

ity under generated text images. TSAP measures whether the predicted anomalous character count  $N_a$  lies within the interval  $[\delta \times N'_a, N'_a/\delta]$ , where  $\delta$  is a tolerance hyperparameter set to 0.7, with such interval-matched cases used to compute Precision, Recall, and F1-scores. For CTR, we report two metrics: Recall and NED for fine-grained assessment. Evaluations are conducted on the test set proposed in Sec. 3.2.2.

For Text Rendering tasks, we first evaluate models on three established benchmarks: OneIG-Bench [6], CVTG-2K [14], and LongText-Bench [20]. We identified that their reliance on structurally-unaware OCR Models [1, 15] can yield unreliable metrics, a critical limitation shared by a broader range of prominent benchmarks [49, 54, 66]. To address this, we first re-evaluate these benchmarks using TextPecker, reporting both semantic alignment scores and structural quality scores (defined in Sec. 3.2.1 with  $\omega = 1$  for evaluation). To streamline this re-evaluation with TextPecker and leverage the strengths of existing benchmarks, we integrate English and Chinese prompts curated from these datasets [6, 14, 20, 49, 55, 66], referred to as *GenTextEval* for brevity. Given the scarcity of Chinese-rendering benchmarks [6, 20, 55], we supplement this integrated set with Chinese prompts constructed in Sec. 3.2.2, resulting in a total of 314 English prompts and 417 Chinese prompts. More details are provided in the Appendix.

**Baselines.** We compare TextPecker against both specialist OCR models and general MLLMs. The former includes PPOCRv5 [15], GOT-OCR-2.0 [53], MonkeyOCR [31]. For the latter, we benchmark against leading proprietary models such as GPT-5 [40], Gemini-2.5-Pro [11], and Doubao-Seed-1.6 [4, 5], as well as strong open-source alternatives like Qwen3-VL [60] and InternVL3[69].

### 4.2. Main Results

Additional results on evaluator generalization, RL baselines, multi-reward and ablations are presented in the appendix.

#### 4.2.1. Quantitative Results

**TSAP and CTR.** As illustrated in Tab. 2, our quantitative analysis reveals significant limitations in existing models and highlights the superiority of TextPecker.

First, we observe a near-total failure of both leading MLLMs and specialist OCR models on the Text Structural Anomaly Perception (TSAP) task. While a few MLLMs like Doubao-Seed-1.6 [4], GPT-5 [40], and InternVL3 [69] show a nascent ability for structural anomaly perception, their performance remains rudimentary. This failure stems from a core mismatch in task nature: (1) these models are trained for generalized text recognition, which prioritizes robust semantic extraction over structural authenticity; for instance, when facing text partially visible due to occlusion, they are encouraged to predict the complete semantics corresponding

Table 2. Results of Text Structural Anomaly Perception (TSAP) and Canonical Text Recognition (CTR): measuring model’s recognition ability under generated text images and TSAP-demanding prompts. Box-level results of non-supporting models are marked as ”-”.

Methods	TSAP						CTR			
	Image-level			Box-level			Image-level		Box-level	
	P	R	F1	P	R	F1	R	NED	R	NED
<i>English recognition</i>										
PP-OCRv5 [15]	0.000	0.000	0.000	-	-	-	0.720	0.137	-	-
GOT-OCR-2.0 [53]	0.000	0.000	0.000	-	-	-	0.610	0.186	-	-
MonkeyOCR [31]	0.000	0.000	0.000	-	-	-	0.578	0.209	-	-
Gemini-2.5-pro [11]	0.179	0.076	0.107	0.342	0.179	0.235	0.415	0.557	0.300	0.571
Doubao-Seed-1.6 [4]	0.157	0.167	0.162	0.333	0.180	0.234	0.714	0.169	0.376	0.473
Doubao-Seed-1.6-think [5]	0.259	0.183	0.214	0.280	0.095	0.141	0.736	0.119	0.418	0.414
GPT-5 [40]	0.196	0.150	0.170	0.419	0.193	0.265	0.556	0.359	0.398	0.450
Qwen3-VL-8B [60]	0.286	0.017	0.032	0.500	0.018	0.034	0.807	0.078	0.761	0.112
InternVL3-8B [69]	0.206	0.165	0.183	0.218	0.443	0.293	0.759	0.102	0.551	0.302
TextPecker (InternVL3-8B) [69]	<b>0.795</b>	0.960	<b>0.870</b>	<b>0.784</b>	<b>0.964</b>	<b>0.865</b>	<b>0.944</b>	<b>0.035</b>	<b>0.953</b>	<b>0.030</b>
TextPecker (Qwen3-VL-8B) [60]	0.777	<b>0.969</b>	0.862	0.714	0.938	0.811	0.918	0.046	0.941	0.038
<i>Chinese recognition</i>										
PP-OCRv5 [15]	0.300	0.013	0.024	-	-	-	0.921	0.067	-	-
GOT-OCR-2.0 [53]	0.500	0.004	0.008	-	-	-	0.853	0.136	-	-
MonkeyOCR [31]	<b>1.000</b>	0.013	0.025	-	-	-	0.917	0.076	-	-
Gemini-2.5-pro [11]	0.079	0.048	0.059	0.333	0.099	0.152	0.574	0.422	0.526	0.473
Doubao-Seed-1.6 [4]	0.306	0.182	0.228	0.310	0.115	0.168	0.918	0.079	0.677	0.322
Doubao-Seed-1.6-think [5]	0.216	0.084	0.121	0.333	0.086	0.137	0.915	0.080	0.758	0.242
GPT-5 [40]	0.233	0.220	0.226	0.282	0.165	0.209	0.758	0.239	0.729	0.270
Qwen3-VL-8B [60]	0.400	0.008	0.017	0.000	0.000	0.000	0.943	0.054	0.931	0.068
InternVL3-8B [69]	0.190	0.128	0.153	0.129	0.370	0.191	0.927	0.069	0.729	0.270
TextPecker (InternVL3-8B) [69]	0.889	0.968	<b>0.927</b>	<b>0.912</b>	<b>0.988</b>	<b>0.949</b>	0.962	0.037	<b>0.991</b>	<b>0.009</b>
TextPecker (Qwen3-VL-8B) [60]	0.874	<b>0.981</b>	0.925	0.900	0.964	0.931	<b>0.972</b>	<b>0.027</b>	0.989	0.010

Table 3. Quantitative comparisons of different RL-optimized generative models on OneIG-Bench [6], LongText-Bench [20], CVTG-2k [14], and GenTextEval-Bench. **Avg.**: Average text score from original benchmarks; **Qua.**: structural Quality score. **Sem.**: Semantic alignment. Score measurement and reward computation are both conducted by TextPecker (Qwen3-VL).

Models	Rewards	OneIG			LongText			CVTG-2K			GenTextEval	
		Avg.	Qua.	Sem.	Avg.	Qua.	Sem.	Avg.	Qua.	Sem.	Qua.	Sem.
<i>English Rendering</i>												
SD3.5-M [16]	-	0.441	0.848	0.513	0.296	0.860	0.416	0.368	0.869	0.491	0.671	0.265
	OCR	0.572	0.941	0.627	0.295	0.944	0.498	0.513	0.943	<b>0.671</b>	0.940	0.462
	TextPecker	<b>0.581</b>	<b>0.957</b>	<b>0.636</b>	<b>0.344</b>	<b>0.957</b>	<b>0.503</b>	<b>0.596</b>	<b>0.944</b>	0.593	<b>0.959</b>	<b>0.506</b>
Flux.1[dev] [28]	-	0.567	0.875	0.585	0.613	0.929	0.591	0.491	0.908	0.523	0.672	0.336
	OCR	0.754	0.969	0.708	0.736	0.972	0.707	<b>0.778</b>	0.951	0.632	0.976	0.602
	TextPecker	<b>0.845</b>	<b>0.979</b>	<b>0.734</b>	<b>0.811</b>	<b>0.986</b>	0.672	0.777	<b>0.961</b>	<b>0.704</b>	<b>0.988</b>	<b>0.719</b>
Qwen-Image [55]	-	0.871	0.955	0.814	0.935	0.970	0.844	0.834	0.964	0.817	0.964	0.729
	OCR	0.986	0.983	0.894	<b>0.949</b>	0.986	0.912	0.893	0.978	0.908	0.989	0.827
	TextPecker	<b>0.990</b>	<b>0.988</b>	<b>0.910</b>	0.945	<b>0.990</b>	<b>0.918</b>	<b>0.899</b>	<b>0.987</b>	<b>0.932</b>	<b>0.992</b>	<b>0.837</b>
<i>Chinese Rendering</i>												
Qwen-Image [55]	-	0.954	0.894	0.732	0.920	0.924	0.834	-	-	-	0.933	0.810
	OCR	0.984	0.945	0.856	0.967	0.956	0.886	-	-	-	0.953	0.874
	TextPecker	<b>0.988</b>	<b>0.956</b>	<b>0.875</b>	<b>0.974</b>	<b>0.969</b>	<b>0.908</b>	-	-	-	<b>0.973</b>	<b>0.897</b>

to their expected full structure rather than verify structural fidelity (Fig. 1). Moreover, generated text frequently contains diverse structural anomalies that are rarely encountered in standard text recognition scenarios.

Besides, we identify a widespread deficiency in box-level text recognition. While traditional OCR models fundamentally lack the ability to process region-specific inputs, modern MLLMs also struggle with structural-anomaly detection. As shown in Tab. 2, their box-level recognition recall is substantially lower than their image-level counterparts. This

limitation severely hinders more fine-grained assessments, which are crucial for evaluating demanding tasks such as controllable text editing and translation of text in local areas. In stark contrast, TextPecker’s models excel across all dimensions. They not only achieve high F1 and recall on the TSAP task but also improve recognition of generated text (CTR) compared to their respective baselines, underscoring the value of our box-level structure-aware dataset. Specifically, the Qwen3-VL-based variant attains state-of-the-art Chinese recognition performance, while the InternVL3-based variant



用于图像识别的深度学习  
作者名单：何恺明，张祥雨，任少卿，孙剑  
摘要：我们提出一种神经网络深度更大的网络训练，以简化比之前使用的网络深度更大的网络训练。我们明确地将层重构建为参考层输入来学习残差函数，而不是学习无参考的函数。我们提供了全面的实证证据，显示残差网络更易优化，且即使深度显著增加也能提升准确性。在ImageNet数据集上，我们评估了深度高达152层的残差网络——其深度是VGG网络[41]的8倍，但复杂性仍然较低。这些残差网络的集合在ImageNet测试集上达到3.57%的准确率。该结果在ILSVRC 2015分类任务中获得第一名。我们还在CIFAR-10上对100层和1000层进行了分析。对于许多视觉识别任务而言，表示的深度具有重要意义。仅因我们极深的表示，我们在COCO目标检测数据集上获得了28%的相对改善。

题：论入顶层性质是差；图像识别的深度学习作者名单：何恺明，张祥雨，任少卿，孙剑  
摘要：更深的神经网络更难训练。我们提出一种深度学习框架，以简化比之前使用的网络深度更大的网络训练。我们明确地将层重构建为参考层输入来学习残差函数，且即使深度显著增加也能提升准确性。我们提供了全面的实证证据，显示残差网络更易优化，且即使深度显著增加也能提升准确性。在ImageNet数据集上，我们评估了深度高达152层的残差网络——其深度是VGG网络[41]的8倍，但复杂性仍然较低。这些残差网络的集合在ImageNet测试集上达到3.57%的准确率。该结果在ILSVRC 2015分类任务中获得第一名。我们还在CIFAR-10上对100层和1000层进行了分析。对于许多视觉识别任务而言，表示的深度具有重要意义。仅因我们极深的表示，我们在COCO目标检测数据集上获得了28%的相对改善。

用于图像识别深度学习  
作者名单：何恺明，张祥雨，任少卿，孙剑  
摘要：更深的神经网络更难训练。我们提出一种深度学习框架，以简化比之前使用的网络深度更大的网络训练。我们明确地将层重构建为参考层输入来学习残差函数，而不是学习无参考的函数。我们提供了全面的实证证据，显示残差网络更易优化，且即使深度显著增加也能提升准确性。在ImageNet数据集上，我们评估了深度高达152层的残差网络——其深度是VGG网络[41]的8倍，但复杂性仍然较低。这些残差网络的集合在ImageNet测试集上达到3.57%的准确率。该结果在ILSVRC 2015分类任务中获得第一名。我们还在CIFAR-10上对100层和1000层进行了分析。对于许多视觉识别任务而言，表示的深度具有重要意义。仅因我们极深的表示，我们在COCO目标检测数据集上获得了28%的相对改善。

“用于图像识别的深度学习作者名单：何恺明，张祥雨，任少卿，孙剑  
摘要：更深的神经网络更难训练。我们提出一种深度学习框架，以简化比之前使用的网络深度更大的网络训练。我们明确地将层重构建为参考层输入来学习残差函数，而不是学习无参考的函数。我们提供了全面的实证证据，显示残差网络更易优化，且即使深度显著增加也能提升准确性。在ImageNet数据集上，我们评估了深度高达152层的残差网络——其深度是VGG网络[41]的8倍，但复杂性仍然较低。这些残差网络的集合在ImageNet测试集上达到3.57%的准确率。该结果在ILSVRC 2015分类任务中获得第一名。我们还在CIFAR-10上对100层和1000层进行了分析。对于许多视觉识别任务而言，表示的深度具有重要意义。仅因我们极深的表示，我们在COCO目标检测数据集上获得了28%的相对改善。”

“EXPLORE THE FUTURE OF ELECTRIC VEHICLES TODAY”, “Visit EVExpo2023.com for details”, “Parking Ahead”, “Turn Right for Downtown”  
“Golden Dragon Restaurant”, “Appetizers”, “Main Courses”, “Spring Rolls – Crispy rolls filled with fresh vegetables \$5”, “Kung Pao Chicken – Stir-fried chicken with peanuts and chili peppers \$14”, “Mango Pudding \$6”, “Jasmine Tea \$3”

Figure 4. Qualitative Comparisons of Text Rendering for Qwen-Image and RL-Optimized Variants. Readers are highly recommended to refer to the appendix for extensive comparisons across generative models and RL baselines.

exhibits the strongest overall capabilities at the box level.

**RL for VTR.** Tab. 3 quantifies the effectiveness of our RL-based optimization across diverse scenarios. Overall, integrating TextPecker’s structure-aware reward yields consistent improvements across four benchmarks, three base models, and both English and Chinese rendering tasks. For Flux.1[dev] [28] on English, gains are pronounced: +38.3% Sem. and +31.6% Qua. over the base model, and +11.7% Sem. over the OCR-reward baseline on GenTextEval. While gains are consistent overall, we also observe a few seemingly contradictory results when evaluated by different metrics. For example, SD3.5-M [16] on CVTG-2K reports +8.3%

average word accuracy across five regions, yet -7.8% Sem. compared to the OCR-reward baseline. This divergence indicates that structure-unaware, OCR-based metrics can overestimate performance on structurally flawed text, underscoring the necessity of a structure-aware assessor for faithful evaluation—despite these localized divergences, the overall benchmark averages still show marked improvement. Notably, even for the well-optimized Qwen-Image [55], TextPecker-based RL delivers significant improvements, especially on Chinese rendering: +14.3% on OneIG, +7.4% on LongText, and +8.7% on GenTextEval over prior SOTA; compared to the OCR-reward baseline, Qua. increases by +2.0% and Sem. by +2.3%. Taken together, these results establish

Table 4. Ablation study on effectiveness of the constructed data: Image-level recognition results across different baseline models.

Models	Settings		English					Chinese				
	Anno.	Syn.	TSAP			CTR		TSAP			CTR	
			P	R	F1	R	NED	P	R	F1	R	NED
InternVL3 [69]	✓		0.206	0.165	0.183	0.759	0.102	0.190	0.128	0.153	0.927	0.069
		✓	<b>0.795</b>	<b>0.970</b>	<b>0.874</b>	0.938	0.042	0.583	0.966	0.727	0.849	0.148
	✓	✓	0.795	0.960	0.870	<b>0.944</b>	<b>0.035</b>	<b>0.889</b>	<b>0.968</b>	<b>0.927</b>	<b>0.962</b>	<b>0.037</b>
Qwen3-VL [60]	✓		0.182	0.018	0.032	0.810	0.076	0.333	0.008	0.017	0.947	0.049
		✓	0.706	0.944	0.808	0.899	0.068	0.643	0.942	0.764	0.839	0.117
	✓	✓	0.777	0.969	0.862	<b>0.918</b>	<b>0.046</b>	<b>0.874</b>	<b>0.981</b>	<b>0.925</b>	<b>0.972</b>	<b>0.027</b>

TextPecker as a generalizable, plug-and-play reward that advances structurally faithful and accurate text rendering.

### 4.2.2. Qualitative Results

We present qualitative comparisons for Qwen-Image and its RL-optimized variants in Fig. 4. The vanilla Qwen-Image, despite achieving prior SOTA on several text rendering benchmarks, often produces off-target strings and exhibits blurred, distorted, or misaligned text, particularly in small and dense text regions. Optimizing with an OCR-based reward helps reducing off-target content and semantic alignment is enhanced, yet structural defects persist. In contrast, TextPecker-based RL achieves superior structural fidelity and semantic consistency (*e.g.* the English menu and Chinese paper cases). These observations align with the quantitative gains in Tab. 3 and the component analysis in Tab. 5, and we observe similar trends across other backbones (see Appendix), underscoring TextPecker’s effectiveness as a reward for structurally faithful and accurate text rendering.

In stark contrast, further optimization with TextPecker achieves a superior level of both structural fidelity and semantic consistency. This is particularly evident in challenging cases where OCR-based rewards falter. For instance, in the “paper rendering” case, our method successfully renders clean, aligned paragraphs where the OCR-rewarded model still produces distorted and wavy text lines. Similarly, in the “English menu” example, TextPecker accurately generates crisp, legible items that the baseline struggles to form correctly.

### 4.3. Ablation Studies

We conduct ablation studies to validate the effectiveness of our proposed dataset and to dissect the contribution of each component within the TextPecker reward mechanism.

**Effectiveness of Data Composition.** As shown in Tab. 4, training on our annotated data alone yields substantial improvements on the TSAP task, with F1 scores for both models significantly outperforming the baseline. This data also enhances English text recognition. However, we observe a noticeable degradation in Chinese recognition performance, which we attribute to the increased complexity of structural anomalies in Chinese characters. The addition of our synthesized data effectively resolves this issue. By training on a

Table 5. Ablation study on the effectiveness of reward design: PM for Pair-wise Matching, and SQ for Structural Quality reward.

Generative Model	OCR Model	Settings			GenTextEval-EN	
		NED	PM	SQ	Qua.	Sem.
Flux.1[dev] [28]	-				0.672	0.336
	PP-OCRv5 [15]	✓			0.976	0.602
	PP-OCRv5 [15]	✓	✓		0.976	0.644
	TextPecker	✓	✓	✓	0.984	0.702
	TextPecker	✓	✓	✓	<b>0.988</b>	<b>0.719</b>

combined dataset, both models demonstrate a dramatic boost in Chinese performance for both TSAP and CTR, achieving precise recognition and high accuracy in detecting structural anomalies. For English, the impact is model-dependent: while Qwen3-VL shows consistent enhancement, InternVL3 exhibits a slight decline in TSAP performance, yet gains notable improvements in CTR.

**Analysis of Reward Components.** We deconstruct the reward function step-by-step to isolate the impact of each component. As shown in Tab. 5, combining a conventional, structure-unaware OCR model with Pairwise Matching (PM) yields a 4.2% gain in the semantic alignment score, yet the structural quality score remains stagnant—indicating that GNED sharpens semantic feedback but fails to improve structural fidelity when the recognizer lacks structural perception. Replacing the OCR model with TextPecker delivers gains across both dimensions (Sem. +5.8%, Qua. +0.8%), as TextPecker’s reward is **inherently structure-aware**: characters identified with special markers directly modulate the semantic score. Finally, incorporating the structural quality term as an auxiliary reward brings further improvements and achieves the best overall performance, confirming the synergy of the full TextPecker reward design.

## 5. Conclusion

We pinpoint and address the core bottleneck in VTR evaluation and RL-based optimization: leading MLLMs and specialist OCR models largely fail to perceive fine-grained structural anomalies. We present TextPecker, a plug-and-play, structural-anomaly-aware framework that couples a standardized evaluator with an RL reward, providing complementary reward signals for semantic alignment and structural quality. Empirically, TextPecker delivers consistent gains across leading text-to-image generators, including notable improvements on the well-optimized Qwen-Image. Under structure-aware rewards, generation behavior shifts toward fewer off-target strings, reduced blur and distortion, and improved alignment. This work provides a foundational step towards structurally faithful visual text rendering and supplies the community with essential tools for rigorous evaluation and post-training enhancement.

## References

- [1] Shuai Bai, Keqin Chen, Xuejing Liu, Jialin Wang, Wenbin Ge, Sibao Song, Kai Dang, Peng Wang, Shijie Wang, Jun Tang, Humen Zhong, Yuanzhi Zhu, Mingkun Yang, Zhaohai Li, Jianqiang Wan, Pengfei Wang, Wei Ding, Zheren Fu, Yiheng Xu, Jiabo Ye, Xi Zhang, Tianbao Xie, Zesen Cheng, Hang Zhang, Zhibo Yang, Haiyang Xu, and Junyang Lin. Qwen2.5-vl technical report. *arXiv preprint arXiv:2502.13923*, 2025. 1, 2, 3, 5
- [2] James Betker, Gabriel Goh, Li Jing, Tim Brooks, Jianfeng Wang, Linjie Li, Long Ouyang, Juntang Zhuang, Joyce Lee, Yufei Guo, et al. Improving image generation with better captions. *Computer Science*. <https://cdn.openai.com/papers/dall-e-3.pdf>, 2(3):8, 2023. 1
- [3] ByteDance. Seedream4.0. [https://seed.bytedance.com/en/seedream4\\_0](https://seed.bytedance.com/en/seedream4_0), 2025. Accessed: 2025-09-22. 1, 2, 3
- [4] ByteDance. Doubao-seed-1.6. [https://seed.bytedance.com/en/seed1\\_6](https://seed.bytedance.com/en/seed1_6), 2025. Accessed: 2025-09-22. 5, 6
- [5] ByteDance. Doubao-seed-1.6-thinking. [https://seed.bytedance.com/en/seed1\\_6](https://seed.bytedance.com/en/seed1_6), 2025. Accessed: 2025-09-22. 5, 6
- [6] Jingjing Chang, Yixiao Fang, Peng Xing, Shuhan Wu, Wei Cheng, Rui Wang, Xianfang Zeng, Gang Yu, and Hai-Bao Chen. Oneig-bench: Omni-dimensional nuanced evaluation for image generation. *arXiv preprint arxiv:2506.07977*, 2025. 1, 2, 5, 6, 12, 14, 16, 17
- [7] Jingye Chen, Yupan Huang, Tengchao Lv, Lei Cui, Qifeng Chen, and Furu Wei. Textdiffuser: Diffusion models as text painters. *NIPS*, 36:9353–9387, 2023. 2
- [8] Jingye Chen, Yupan Huang, Tengchao Lv, Lei Cui, Qifeng Chen, and Furu Wei. Textdiffuser-2: Unleashing the power of language models for text rendering. In *ECCV*, pages 386–402. Springer, 2024. 2
- [9] Jiu hai Chen, Le Xue, Zhiyang Xu, Xichen Pan, Shusheng Yang, Can Qin, An Yan, Honglu Zhou, Zeyuan Chen, Lifu Huang, et al. Blip3o-next: Next frontier of native image generation. *arXiv preprint arXiv:2510.15857*, 2025. 1, 3
- [10] Gheorghe Comanici, Eric Bieber, Mike Schaekermann, Ice Pasupat, Noveen Sachdeva, Inderjit Dhillon, Marcel Blistein, Ori Ram, Dan Zhang, Evan Rosen, et al. Gemini 2.5: Pushing the frontier with advanced reasoning, multimodality, long context, and next generation agentic capabilities. *arXiv preprint arXiv:2507.06261*, 2025. 1, 18
- [11] Gheorghe Comanici, Eric Bieber, Mike Schaekermann, Ice Pasupat, Noveen Sachdeva, Inderjit Dhillon, Marcel Blistein, Ori Ram, Dan Zhang, Evan Rosen, et al. Gemini 2.5: Pushing the frontier with advanced reasoning, multimodality, long context, and next generation agentic capabilities. *arXiv preprint arXiv:2507.06261*, 2025. 5, 6, 12, 13
- [12] Chaorui Deng, Deyao Zhu, Kunchang Li, Chenhui Gou, Feng Li, Zeyu Wang, Shu Zhong, Weihao Yu, Xiaonan Nie, Ziang Song, et al. Emerging properties in unified multimodal pre-training. *arXiv preprint arXiv:2505.14683*, 2025. 1, 2
- [13] Ming Ding, Zhuoyi Yang, Wenyi Hong, Wendi Zheng, Chang Zhou, Da Yin, Junyang Lin, Xu Zou, Zhou Shao, Hongxia Yang, et al. Cogview: Mastering text-to-image generation via transformers. *NIPS*, 34:19822–19835, 2021. 4, 15
- [14] Nikai Du, Zhennan Chen, Shan Gao, Zhizhou Chen, Xi Chen, Zhengkai Jiang, Jian Yang, and Ying Tai. Textcrafter: Accurately rendering multiple texts in complex visual scenes. *arXiv preprint arXiv:2503.23461*, 2025. 1, 2, 5, 6, 14, 16, 17
- [15] Yuning Du, Chenxia Li, Ruoyu Guo, Xiaoting Yin, Weiwei Liu, Jun Zhou, Yifan Bai, Zilin Yu, Yehua Yang, Qingqing Dang, et al. Pp-ocr: A practical ultra lightweight ocr system. *arXiv preprint arXiv:2009.09941*, 2020. 1, 2, 3, 4, 5, 6, 8, 12, 17
- [16] Patrick Esser, Sumith Kulal, Andreas Blattmann, Rahim Entezari, Jonas Müller, Harry Saini, Yam Levi, Dominik Lorenz, Axel Sauer, Frederic Boesel, et al. Scaling rectified flow transformers for high-resolution image synthesis. In *ICML*, 2024. 2, 4, 5, 6, 7, 12, 14, 15, 16, 17
- [17] Rongyao Fang, Aldrich Yu, Chengqi Duan, Linjiang Huang, Shuai Bai, Yuxuan Cai, Kun Wang, Si Liu, Xihui Liu, and Hongsheng Li. Flux-reason-6m & prism-bench: A million-scale text-to-image reasoning dataset and comprehensive benchmark. *arXiv preprint arXiv:2509.09680*, 2025. 2
- [18] Yu Gao, Lixue Gong, Qiushan Guo, Xiaoxia Hou, Zhichao Lai, Fanshi Li, Liang Li, Xiaochen Lian, Chao Liao, Liyang Liu, et al. Seedream 3.0 technical report. *arXiv preprint arXiv:2504.11346*, 2025. 1, 3, 4, 15
- [19] Yifan Gao, Zihang Lin, Chuanbin Liu, Min Zhou, Tiezheng Ge, Bo Zheng, and Hongtao Xie. Postermaker: Towards high-quality product poster generation with accurate text rendering. In *CVPR*, pages 8083–8093, 2025. 2
- [20] Zigang Geng, Yibing Wang, Yeyao Ma, Chen Li, Yongming Rao, Shuyang Gu, Zhao Zhong, Qinglin Lu, Han Hu, Xiaosong Zhang, et al. X-omni: Reinforcement learning makes discrete autoregressive image generative models great again. *arXiv preprint arXiv:2507.22058*, 2025. 1, 2, 3, 5, 6, 12, 14, 16, 17
- [21] Lixue Gong, Xiaoxia Hou, Fanshi Li, Liang Li, Xiaochen Lian, Fei Liu, Liyang Liu, Wei Liu, Wei Lu, Yichun Shi, et al. Seedream 2.0: A native chinese-english bilingual image generation foundation model. *arXiv preprint arXiv:2503.07703*, 2025. 3
- [22] Daya Guo, Dejian Yang, Haowei Zhang, Junxiao Song, Peiyi Wang, Qihao Zhu, Runxin Xu, Ruoyu Zhang, Shirong Ma, Xiao Bi, et al. Deepseek-r1 incentivizes reasoning in llms through reinforcement learning. *Nature*, 645(8081):633–638, 2025. 3
- [23] Conghui He, Zhenjiang Jin, Chao Xu, Jiantao Qiu, Bin Wang, Wei Li, Hang Yan, Jiaqi Wang, and Dahua Lin. Wanjuan: A comprehensive multimodal dataset for advancing english and chinese large models. *arXiv preprint arXiv:2308.10755*, 2023. 4, 16
- [24] Zhentao He, Can Zhang, Ziheng Wu, Zhenghao Chen, Yufei Zhan, Yifan Li, Zhao Zhang, Xian Wang, and Minghui Qiu. Seeing is believing? mitigating ocr hallucinations in multimodal large language models. *arXiv preprint arXiv:2506.20168*, 2025. 2
- [25] Yuval Kirstain, Adam Polyak, Uriel Singer, Shahbuland Matiana, Joe Penna, and Omer Levy. Pick-a-pic: An open dataset

- of user preferences for text-to-image generation. *Advances in neural information processing systems*, 36:36652–36663, 2023. 12, 13, 14
- [26] Harold W Kuhn. The hungarian method for the assignment problem. *Naval research logistics quarterly*, 2(1-2):83–97, 1955. 2
- [27] Kwai-Kolors Kolors. Kolors. <https://huggingface.co/Kwai-Kolors/Kolors>, 2025. Accessed: 2025-09-22. 4, 15
- [28] Black Forest Labs. Flux. <https://github.com/black-forest-labs/flux>, 2024. 1, 2, 3, 4, 5, 6, 7, 8, 12, 13, 14, 15, 17, 18
- [29] Yingxin Lai, Cuijie Xu, Haitian Shi, Guoqing Yang, Xiaoning Li, Zhiming Luo, and Shaozi Li. Font-agent: Enhancing font understanding with large language models. In *CVPR*, pages 19670–19680, 2025. 2
- [30] Junzhe Li, Yutao Cui, Tao Huang, Yinping Ma, Chun Fan, Miles Yang, and Zhao Zhong. Mixgrpo: Unlocking flow-based grpo efficiency with mixed ode-sde. *arXiv preprint arXiv:2507.21802*, 2025. 12, 17
- [31] Zhang Li, Yuliang Liu, Qiang Liu, Zhiyin Ma, Ziyang Zhang, Shuo Zhang, Zidun Guo, Jiarui Zhang, Xinyu Wang, and Xiang Bai. Monkeyocr: Document parsing with a structure-recognition-relation triplet paradigm. *arXiv preprint arXiv:2506.05218*, 2025. 5, 6
- [32] Bin Lin, Zongjian Li, Xinhua Cheng, Yuwei Niu, Yang Ye, Xianyi He, Shenghai Yuan, Wangbo Yu, Shaodong Wang, Yunyang Ge, et al. Uniworld: High-resolution semantic encoders for unified visual understanding and generation. *arXiv preprint arXiv:2506.03147*, 2025. 2
- [33] Yaron Lipman, Ricky TQ Chen, Heli Ben-Hamu, Maximilian Nickel, and Matt Le. Flow matching for generative modeling. *arXiv preprint arXiv:2210.02747*, 2022. 3
- [34] Jie Liu, Gongye Liu, Jiajun Liang, Yangguang Li, Jiaheng Liu, Xintao Wang, Pengfei Wan, Di Zhang, and Wanli Ouyang. Flow-grpo: Training flow matching models via online rl. *arXiv preprint arXiv:2505.05470*, 2025. 3, 5, 12, 13, 14, 16
- [35] Xingchao Liu, Chengyue Gong, and Qiang Liu. Flow straight and fast: Learning to generate and transfer data with rectified flow. *arXiv preprint arXiv:2209.03003*, 2022. 3
- [36] Zeyu Liu, Weicong Liang, Yiming Zhao, Bohan Chen, Lin Liang, Lijuan Wang, Ji Li, and Yuhui Yuan. Glyph-byt5-v2: A strong aesthetic baseline for accurate multilingual visual text rendering. *arXiv preprint arXiv:2406.10208*, 2024. 2
- [37] Dongliang Luo, Hanshen Zhu, Ziyang Zhang, Dingkan Liang, Xudong Xie, Yuliang Liu, and Xiang Bai. Semiets: Integrating spatial and content consistencies for semi-supervised end-to-end text spotting. In *Proceedings of the Computer Vision and Pattern Recognition Conference*, pages 9329–9338, 2025. 2
- [38] Jian Ma, Yonglin Deng, Chen Chen, Nanyang Du, Haonan Lu, and Zhenyu Yang. Glyphdraw2: Automatic generation of complex glyph posters with diffusion models and large language models. In *AAAI*, pages 5955–5963, 2025. 2
- [39] OpenAI. Gpt-4o. <https://openai.com/index/hello-gpt-4o>, 2024. Accessed: 2025-09-22. 1
- [40] OpenAI. Gpt-5. <https://openai.com/gpt-5>, 2025. Accessed: 2025-09-22. 2, 5, 6
- [41] Dustin Podell, Zion English, Kyle Lacey, Andreas Blattmann, Tim Dockhorn, Jonas Müller, Joe Penna, and Robin Rombach. SDXL: improving latent diffusion models for high-resolution image synthesis. In *ICLR*, 2024. 1
- [42] Rafael Rafailov, Archit Sharma, Eric Mitchell, Christopher D Manning, Stefano Ermon, and Chelsea Finn. Direct preference optimization: Your language model is secretly a reward model. *Advances in neural information processing systems*, 36:53728–53741, 2023. 3
- [43] Robin Rombach, Andreas Blattmann, Dominik Lorenz, Patrick Esser, and Björn Ommer. High-resolution image synthesis with latent diffusion models. In *CVPR*, pages 10674–10685, 2022. 4, 15
- [44] Chitwan Saharia, William Chan, Saurabh Saxena, Lala Li, Jay Whang, Emily L. Denton, Seyed Kamyar Seyed Ghasemipour, Raphael Gontijo Lopes, Burcu Karagol Ayan, Tim Salimans, Jonathan Ho, David J. Fleet, and Mohammad Norouzi. Photorealistic text-to-image diffusion models with deep language understanding. In *NeurIPS*, 2022. 1
- [45] Christoph Schuhmann. Laion-aesthetics. *LAION Blog*, 2022. 12, 13, 14
- [46] Yichun Shi, Peng Wang, and Weilin Huang. Seedit: Align image re-generation to image editing. *arXiv preprint arXiv:2411.06686*, 2024. 18
- [47] Yuxiang Tuo, Wangmeng Xiang, Jun-Yan He, Yifeng Geng, and Xuansong Xie. Anytext: Multilingual visual text generation and editing. *arXiv preprint arXiv:2311.03054*, 2023. 15, 18
- [48] Yuxiang Tuo, Yifeng Geng, and Liefeng Bo. Anytext2: Visual text generation and editing with customizable attributes. *arXiv preprint arXiv:2411.15245*, 2024. 2
- [49] Alex Jinpeng Wang, Dongxing Mao, Jiawei Zhang, Weiming Han, Zhuobai Dong, Linjie Li, Yiqi Lin, Zhengyuan Yang, Libo Qin, Fuwei Zhang, Lijuan Wang, and Min Li. Textatlas5m: A large-scale dataset for dense text image generation. *arXiv preprint arXiv:2502.07870*, 2025. 2, 4, 5, 14, 16
- [50] Jing Wang, Jiajun Liang, Jie Liu, Henglin Liu, Gongye Liu, Jun Zheng, Wanyuan Pang, Ao Ma, Zhenyu Xie, Xintao Wang, et al. Grpo-guard: Mitigating implicit over-optimization in flow matching via regulated clipping. *arXiv preprint arXiv:2510.22319*, 2025. 12, 17
- [51] Yibin Wang, Yuhang Zang, Hao Li, Cheng Jin, and Jiaqi Wang. Unified reward model for multimodal understanding and generation. *arXiv preprint arXiv:2503.05236*, 2025. 2
- [52] Yibin Wang, Weizhong Zhang, Honghui Xu, and Cheng Jin. Dreamtext: High fidelity scene text synthesis. In *CVPR*, pages 28555–28563, 2025. 2
- [53] Haoran Wei, Chenglong Liu, Jinyue Chen, Jia Wang, Lingyu Kong, Yanming Xu, Zheng Ge, Liang Zhao, Jianjian Sun, Yuang Peng, et al. General ocr theory: Towards ocr-2.0 via a unified end-to-end model. *arXiv preprint arXiv:2409.01704*, 2024. 1, 2, 3, 5, 6
- [54] Xinyu Wei, Jinrui Zhang, Zeqing Wang, Hongyang Wei, Zhen Guo, and Lei Zhang. Tiif-bench: How does your t2i model follow your instructions? *arXiv preprint arXiv:2506.02161*, 2025. 2, 4, 5, 14

- [55] Chenfei Wu, Jiahao Li, Jingren Zhou, Junyang Lin, Kaiyuan Gao, Kun Yan, Sheng-ming Yin, Shuai Bai, Xiao Xu, Yilei Chen, et al. Qwen-image technical report. *arXiv preprint arXiv:2508.02324*, 2025. [1](#), [2](#), [3](#), [4](#), [5](#), [6](#), [7](#), [12](#), [14](#), [15](#), [16](#), [17](#), [18](#)
- [56] Chenyuan Wu, Pengfei Zheng, Ruiran Yan, Shitao Xiao, Xin Luo, Yuezhe Wang, Wanli Li, Xiyan Jiang, Yexin Liu, Junjie Zhou, et al. Omnigen2: Exploration to advanced multimodal generation. *arXiv preprint arXiv:2506.18871*, 2025. [2](#)
- [57] Tianhe Wu, Jian Zou, Jie Liang, Lei Zhang, and Kede Ma. Visualquality-r1: Reasoning-induced image quality assessment via reinforcement learning to rank. *arXiv preprint arXiv:2505.14460*, 2025. [2](#)
- [58] Xiaoshi Wu, Yiming Hao, Keqiang Sun, Yixiong Chen, Feng Zhu, Rui Zhao, and Hongsheng Li. Human preference score v2: A solid benchmark for evaluating human preferences of text-to-image synthesis. *arXiv preprint arXiv:2306.09341*, 2023. [2](#)
- [59] Linting Xue, Aditya Barua, Noah Constant, Rami Al-Rfou, Sharan Narang, Mihir Kale, Adam Roberts, and Colin Raffel. Byt5: Towards a token-free future with pre-trained byte-to-byte models. *Transactions of the Association for Computational Linguistics*, 10:291–306, 2022. [2](#)
- [60] An Yang, Anfeng Li, Baosong Yang, Beichen Zhang, Binyuan Hui, Bo Zheng, Bowen Yu, Chang Gao, Chengen Huang, Chenxu Lv, et al. Qwen3 technical report. *arXiv preprint arXiv:2505.09388*, 2025. [1](#), [4](#), [5](#), [6](#), [8](#), [16](#)
- [61] Yukang Yang, Dongnan Gui, Yuhui Yuan, Weicong Liang, Haisong Ding, Han Hu, and Kai Chen. Glyphcontrol: Glyph conditional control for visual text generation. *Advances in Neural Information Processing Systems*, 36:44050–44066, 2023. [2](#)
- [62] Moonbin Yim, Yoonsik Kim, Han-Cheol Cho, and Sungrae Park. Synthtiger: Synthetic text image generator towards better text recognition models. In *International conference on document analysis and recognition*, pages 109–124. Springer, 2021. [5](#), [15](#)
- [63] Weichao Zeng, Yan Shu, Zhenhang Li, Dongbao Yang, and Yu Zhou. Textctrl: Diffusion-based scene text editing with prior guidance control. *NIPS*, 37:138569–138594, 2024. [2](#)
- [64] Lingjun Zhang, Xinyuan Chen, Yaohui Wang, Yue Lu, and Yu Qiao. Brush your text: Synthesize any scene text on images via diffusion model. In *AAAI*, pages 7215–7223, 2024. [2](#)
- [65] Peirong Zhang, Haowei Xu, Jiabin Zhang, Guitao Xu, Xuhan Zheng, Zhenhua Yang, Junle Liu, Yuyi Zhang, and Lianwen Jin. Aesthetics is cheap, show me the text: An empirical evaluation of state-of-the-art generative models for ocr. *arXiv preprint arXiv:2507.15085*, 2025. [1](#), [2](#)
- [66] Shitian Zhao, Qilong Wu, Xinyue Li, Bo Zhang, Ming Li, Qi Qin, Dongyang Liu, Kai Zhang, Hongsheng Li, Yu Qiao, Peng Gao, Bin Fu, and Zhen Li. Lex-art: Rethinking text generation via scalable high-quality data synthesis. *arXiv preprint arXiv:2503.21749*, 2025. [2](#), [4](#), [5](#), [14](#)
- [67] Yiming Zhao and Zhouhui Lian. Udifftext: A unified framework for high-quality text synthesis in arbitrary images via character-aware diffusion models. In *ECCV*, pages 217–233. Springer, 2024. [2](#)
- [68] Hanshen Zhu, Zhen Zhu, Kaile Zhang, Yiming Gong, Yuliang Liu, and Xiang Bai. Training-free geometric image editing on diffusion models. In *Proceedings of the IEEE/CVF International Conference on Computer Vision*, pages 19130–19140, 2025. [18](#)
- [69] Jinguo Zhu, Weiyun Wang, Zhe Chen, Zhaoyang Liu, Shenglong Ye, Lixin Gu, Hao Tian, Yuchen Duan, Weijie Su, Jie Shao, et al. Internvl3: Exploring advanced training and test-time recipes for open-source multimodal models. *arXiv preprint arXiv:2504.10479*, 2025. [1](#), [5](#), [6](#), [8](#), [12](#)

# TextPecker: Rewarding Structural Anomaly Quantification for Enhancing Visual Text Rendering (Supplementary Materials)

## A. Additional Results

We provide additional visualizations of manually annotated structural anomalies from diverse generative models and synthetic structural anomalies generated by our rendering engine in Fig. 12, evaluation samples of TextPecker in Fig. 13, and qualitative comparisons between Flux.1[dev] [28] and its RL-optimized variants in Fig. 5.

## B. Additional Ablation Studies

Table 6. Ablation study on the effectiveness of reward design: PM for Pair-wise Matching, and SQ for Structural Quality reward, measured by TextPecker (InternVL3).

Generative Model	OCR Model	Settings			GenTextEval-EN	
		NED	PM	SQ	Qua.	Sem.
SD3.5-M [16]	-				0.671	0.265
	PP-OCRv5 [15]	✓			0.907	0.470
	PP-OCRv5 [15]	✓	✓		0.910	0.482
	TextPecker	✓	✓		0.956	0.498
	TextPecker	✓	✓	✓	<b>0.959</b>	<b>0.506</b>

We also provide additional ablation studies to deconstruct the reward function step-by-step and isolate the impact of each component, using StableDiffusion3.5-Medium [16] as the baseline, as shown in Tab. 6. Combining a conventional, structure-unaware OCR model with Pairwise Matching (PM) yields a 1.2% gain in semantic alignment, while structural quality sees a marginal 0.3% improvement—indicating PM enhances semantic feedback but minimally boosts structural fidelity without structural perception. Replacing the OCR model with TextPecker delivers gains across both dimensions (Sem. +1.6%, Qua. +4.6%), demonstrating the value of our structure-aware assessor. Finally, incorporating the structural quality term as an auxiliary reward brings further improvements (Sem. +0.8%, Qua. +0.3%) and achieves the best overall performance, confirming the synergy of the full TextPecker reward design.

## C. Additional Generalization Results

We conduct **cross-model validation** on Gemini-2.5-flash-image [11] renderings to assess robustness under normal and extreme conditions (Tab. 7), and the results are consistent across these settings, with failures mainly on extremely stylized fonts where artistic deformations distort canonical glyph structure and blur the boundary between style and true structural errors (see Fig. 6, cases are all from Gemini). As

for font variability, our dataset spans a large and diverse font pool across training and evaluation (Tab. 14)

Table 7. Robustness evaluation of TextPecker on Gemini-2.5-flash-image [11]: Performance under normal condition, extreme stylization, and low-contrast layouts.

Tab. A & Methods	Normal		Extreme Stylization		Low Contrast	
	TSAP-F1	CTR-R	TSAP-F1	CTR-R	TSAP-F1	CTR-R
InternVL-3-8B [69]	0.000	0.666	0.087	<b>0.588</b>	0.364	0.742
TextPecker-8B	<b>0.752</b>	<b>0.833</b>	<b>0.571</b>	<u>0.577</u>	<b>0.800</b>	<b>0.839</b>

Table 8. Additional Quantitative Comparisons of RL-Optimized Generative Models on **Chinese** Visual Text Benchmarks (OneIG [6], LongText [20], GenTextEval) with multi reward setting. **O**: OCR Reward [34], **S**: TextPecker Semantic Reward, **Q**: TextPecker Structural Quality reward, **P**: Pickscore Reward [25], **A**: Aesthetic Reward [45]. Results measurement and reward computation are both conducted by TextPecker (InternVL-3).

method	rewards	weights	OneIG		LongText		GenTextEval	
			Qua.	Sem.	Qua.	Sem.	Qua.	Sem.
Qwen-Image [55]	-	-	0.888	0.747	0.900	0.815	0.922	0.805
	OPA	7:1:2	0.898	0.788	0.912	0.845	0.944	0.859
	SQPA	5:2:1:2	<b>0.943</b>	<b>0.828</b>	<b>0.941</b>	<b>0.889</b>	<b>0.970</b>	<b>0.893</b>

## D. Additional Results on RL for VTR

To further validate the efficacy of TextPecker and attain more robust performance in Visual Text Rendering, we conduct additional experiments under a **strengthened RL baseline setting**, with key design choices elaborated as follows:

**Backbone enhancement.** We adopt recent GRPO-related techniques[30, 50] to substantially enhance the efficiency and stability of the VTR optimization process, with implementation details supplemented in Sec. G:

- (i) Flow-GRPO-Fast [30] is employed to accelerate training convergence by injecting stochasticity only on partial optimization steps instead of all steps;
- (ii) GRPO-Guard [50] is employed to stabilize the training dynamics and mitigate implicit over-optimization issues in flow matching;
- (iii) KL regularization enhancement (discussed in Flow-GRPO’s [34] GitHub issues) is introduced to further alleviate over-optimization and reward hacking problems. The original formulation is:

$$D_{\text{KL}}(\pi_{\theta} \parallel \pi_{\text{ref}}) = \frac{\|\bar{x}_{t+\Delta t, \theta} - \bar{x}_{t+\Delta t, \text{ref}}\|^2}{2\sigma_t^2 \Delta t}$$

To stabilize training dynamics and mitigate over-optimization more effectively, we redefine the KL divergence

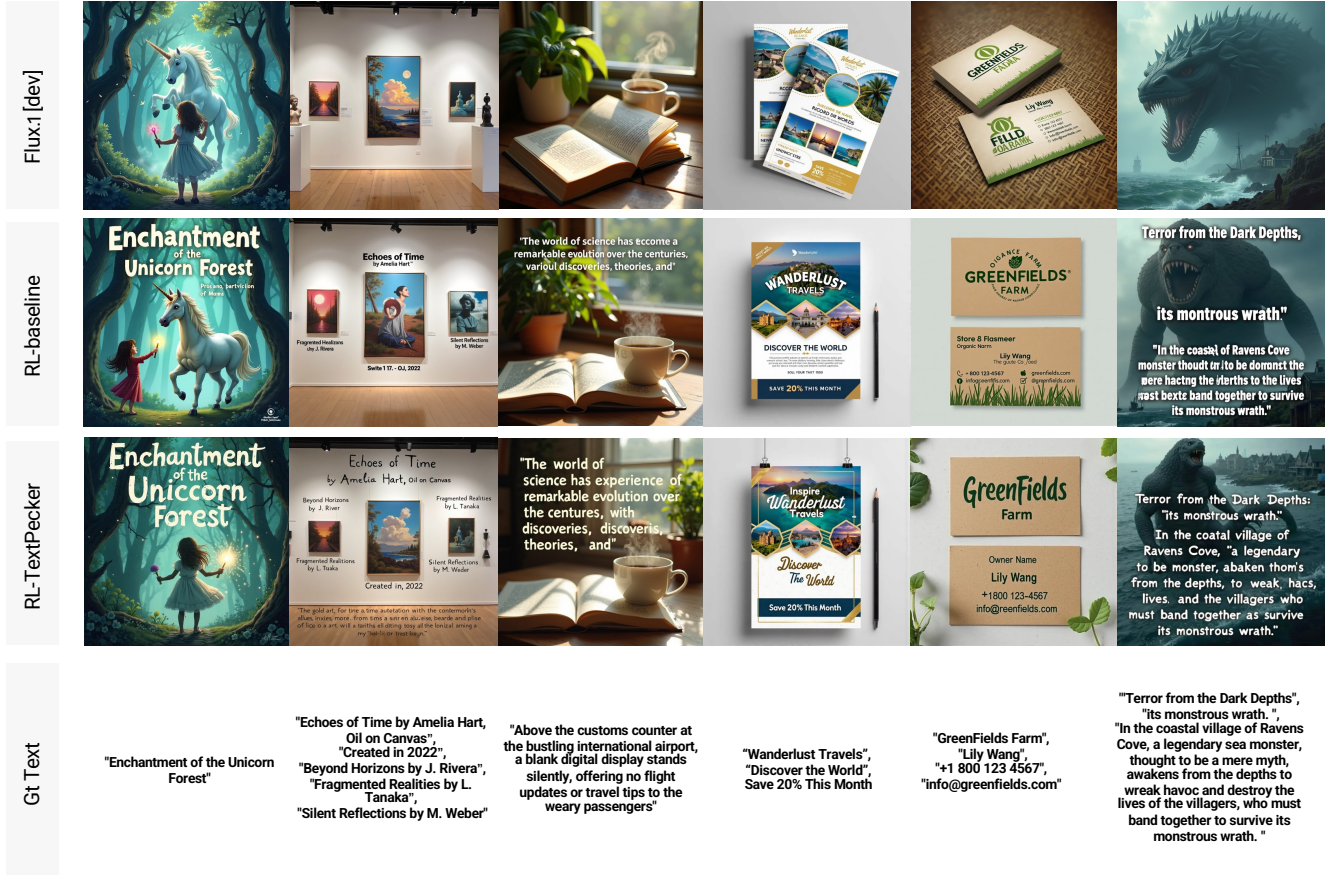


Figure 5. Qualitative Comparisons of Text Rendering for Flux.1 [dev] [28] and RL-Optimized Variants.



Figure 6. Hard Cases of TextPecker on Gemini-Rendered [11] Visual Text with Extreme Stylization and Low Contrast Layout.

to operate over **velocity-based** policy distributions:

$$D_{\text{KL}}(\pi_{\theta} \parallel \pi_{\text{ref}}) = \|v_{\theta}(x_t, t) - v_{\text{ref}}(x_t, t)\|^2$$

where all symbols follow the definitions in the Flow-GRPO [34] paper, with the core adjustment being the switch from state ( $\bar{x}$ ) to velocity ( $v$ ) as the regularization target. **Multi-Reward Regularization.** In the main paper, we validated TextPecker’s efficacy via experiments exclusive to text-rendering rewards. However, this single-reward setup inevitably degrades the model’s aesthetic and image quality performance. To yield more robust VTR optimization, we

propose a multi-reward regularization strategy: we augment the original TextPecker reward with PickScore [25] and Aesthetic Score [45], implicitly regularizing the VTR model to yield more robust RL optimization results.

We present quantitative results of TextPecker under this enhanced RL baseline in Tab. 8 and Tab. 9. Please note that all figures in the main paper and appendix are based on our original RL baseline, except for the additional visual comparisons between the two TextPecker variants provided in Fig. 7 and Fig. 8.

## E. Details of Dataset

### E.1. Details on Text-rich Image Generation

This section supplements the text-rich image generation dataset construction details in the main text. We present detailed statistics on the number of generated images categorized by language and various generative models employed. English dataset statistics in Tab. 10 and Chinese dataset statistics shown in Tab. 11.

Table 9. Additional Quantitative Comparisons of RL-Optimized Generative Models on **English** VTR Benchmarks (OneIG [6], LongText [20], CVTG [14], GenTextEval, TIIF [54], TextAtlas [49], LeX [66]) with multi reward setting. **O**: OCR Reward [34], **S**: TextPecker Semantic Reward, **Q**: TextPecker Structural Quality reward, **P**: Pickscore Reward [25], **A**: Aesthetic Reward [45]. Results measurement and reward computation are both conducted by TextPecker (InternVL-3).

method	rewards	weights	OneIG		LongText		CVTG		GenTextEval		TIIF		TextAtlas		LeX	
			Qua.	Sem.												
SD3.5-M [16]	–	–	0.840	0.507	0.836	0.407	0.843	0.466	0.666	0.262	0.758	0.347	0.646	0.269	0.810	0.454
	OPA	7:1:2	0.908	0.588	0.913	0.508	0.895	<b>0.621</b>	0.896	0.461	0.886	0.483	0.916	0.436	0.894	0.563
	SQPA	5:2:1:2	<b>0.940</b>	<b>0.607</b>	<b>0.959</b>	<b>0.534</b>	<b>0.926</b>	0.587	<b>0.954</b>	<b>0.519</b>	<b>0.941</b>	<b>0.506</b>	<b>0.954</b>	<b>0.462</b>	<b>0.940</b>	<b>0.591</b>
Flux.1[dev] [28]	–	–	0.870	0.578	0.925	0.584	0.889	0.510	0.664	0.332	0.933	0.540	0.683	0.307	0.946	0.667
	OPA	7:1:2	0.977	0.739	0.977	0.763	0.974	0.780	0.982	0.739	0.986	0.719	0.983	0.640	0.988	0.741
	SQPA	5:2:1:2	<b>0.990</b>	<b>0.775</b>	<b>0.992</b>	<b>0.780</b>	<b>0.993</b>	<b>0.824</b>	<b>0.991</b>	<b>0.762</b>	<b>0.991</b>	<b>0.735</b>	<b>0.993</b>	<b>0.649</b>	<b>0.991</b>	<b>0.807</b>
Qwen-Image [55]	–	–	0.954	0.812	0.961	0.831	0.960	0.817	0.958	0.723	0.933	0.682	0.953	0.665	0.927	0.760
	OPA	7:1:2	0.963	0.840	0.967	0.858	0.962	0.848	0.974	0.808	0.964	0.764	0.970	0.728	0.958	0.850
	SQPA	5:2:1:2	<b>0.983</b>	<b>0.888</b>	<b>0.982</b>	<b>0.891</b>	<b>0.976</b>	<b>0.889</b>	<b>0.990</b>	<b>0.876</b>	<b>0.975</b>	<b>0.800</b>	<b>0.982</b>	<b>0.746</b>	<b>0.968</b>	<b>0.883</b>

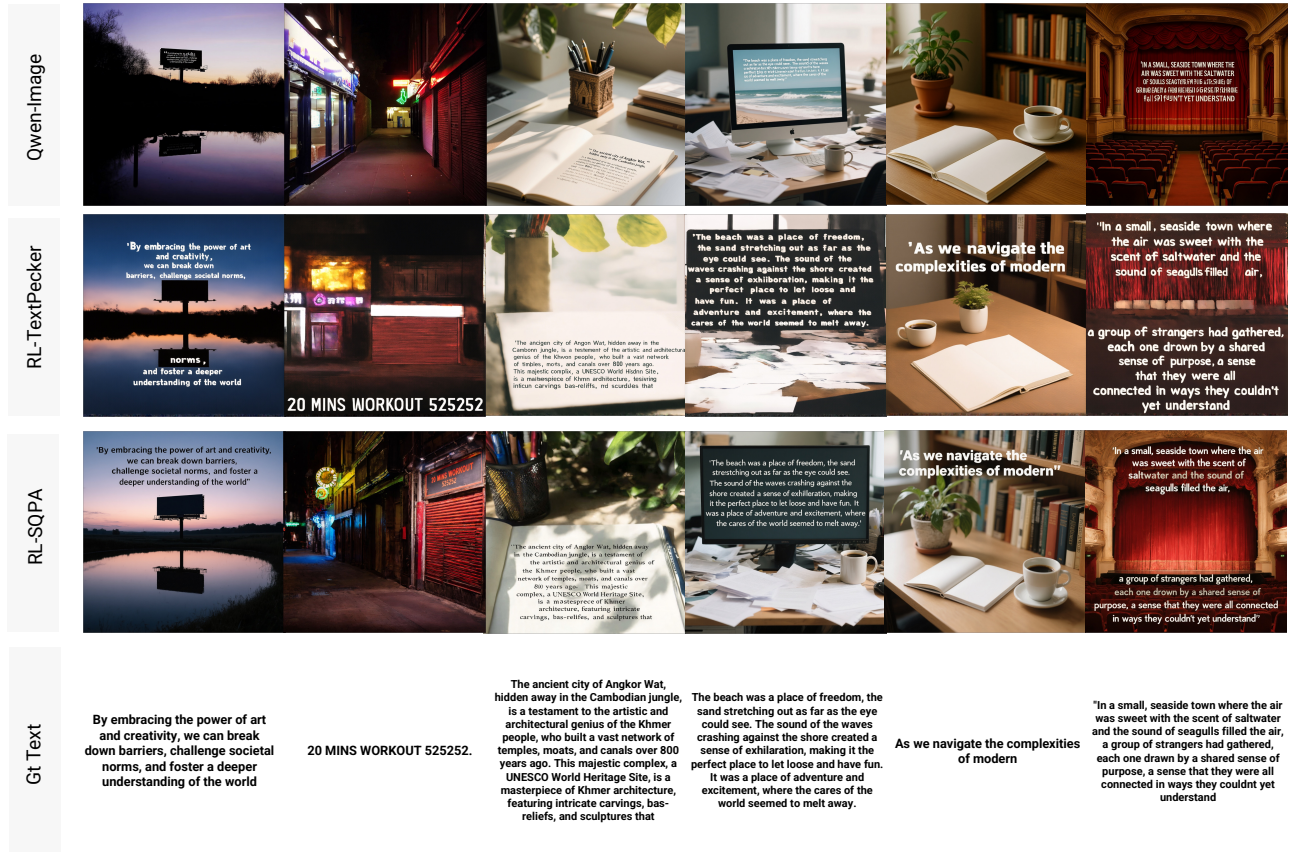


Figure 7. Qualitative comparisons of text rendering results (**English**) among different RL baseline settings. RL-TextPecker denotes the RL setting in the main paper, and RL-SQPA refers to our enhanced RL setting as described in Sec. D.

## E.2. Details on Synthetic Data Augmentation

As demonstrated in the main paper, models trained solely on manually annotated data generalize poorly to unseen struc-

tural anomalies. This limitation is particularly acute for Chinese characters, whose 2D structure and vast inventory (8,000 common characters) create a combinatorial explosion of anomalies impossible to annotate exhaustively. To over-



Figure 8. Qualitative comparisons of text rendering results (Chinese) among different RL baseline settings. RL-TextPecker denotes the RL setting in the main paper, and RL-SQPA refers to our enhanced RL setting as described in Sec. D.

Table 10. Statistics of English text-rich images generated by different models, labeled at box and image levels. Proportions are computed over all instances.

Model	Level	Samples	Proportion
AnyText [47]	Box-level	30647	7.38%
	Image-level	7405	1.78%
Flux.1[dev] [28]	Box-level	91705	22.07%
	Image-level	19181	4.62%
Qwen-Image [55]	Box-level	20308	4.89%
	Image-level	2647	0.64%
SD3 [16]	Box-level	105725	25.45%
	Image-level	17766	4.28%
SDv15 [43]	Box-level	61961	14.91%
	Image-level	6033	1.45%
SeedDream3.0 [18]	Box-level	47921	11.53%
	Image-level	4144	1.00%

come this, we extend the SynthTIGER [62] renderer with two key enhancements: (1) image-level layout arrangements to simulate complex scenes, (2) Structural Anomaly Construction engine tailored to systematically generate diverse

Table 11. Statistics of Chinese text-rich images generated by different models, labeled at box and image levels. Proportions are computed over all instances.

Model	Level	Samples	Proportion
CogView4 [13]	Box-level	36000	11.14%
	Image-level	17005	5.26%
Kolors [27]	Box-level	35549	10.99%
	Image-level	19312	5.98%
Qwen-Image [55]	Box-level	26597	8.23%
	Image-level	6225	1.93%
SeedDream3.0 [18]	Box-level	146395	45.31%
	Image-level	36032	11.15%

structural errors in Chinese.

Key parameters for our rendering engine, covering both canonical text generation and structural anomaly construction, are detailed in Table 14. Our parameter choices are guided by the goal of training precise structural perception, not robust text extraction. Consequently, to preserve clear structural features, we intentionally disabled heavy post-processing (e.g., noise, blur) and certain style effects (e.g.,

extrusion), while limiting geometric transformations (e.g., skew, rotation) to moderate ranges. Notably, we have a **font pool of 976 types** to enhance font diversity. This ensures the rendered text maintains high structural clarity amidst realistic diversity, which is critical for our training objective.

### E.3. Structural Anomaly Perception Test Set

Table 12. Statistics of our constructed text-rich image structural perception test dataset with structural-anomaly labels at box and image levels. Proportions are computed over all instances.

Data Type	Level	Samples	Proportion
Manual Annotations	Box	444	41.85%
	Image	417	39.29%
Synthetic Anomaly Text	Box	50	4.71%
	Image	50	4.71%
Synthetic Normal Text	Box	50	4.71%
	Image	50	4.71%
<b>Total</b>	-	1061	100%

We provide detailed statistics of the structural perception test set in Tab. 12. To further validate the fairness and effectiveness of our results, we additionally conduct evaluations on a **real-only** test split (all synthetic samples excluded), with results presented in Tab. 13.

Table 13. Performance of TextPecker on Real-only Test Splits

Methods	Chinese				English			
	Image		Box		Image		Box	
	TSAP-F1	CTR-R	TSAP-F1	CTR-R	TSAP-F1	CTR-R	TSAP-F1	CTR-R
InternVL3-8B (Baseline)	<b>0.106</b>	<b>0.955</b>	<b>0.244</b>	0.791	<b>0.183</b>	0.759	<b>0.304</b>	0.570
TextPecker-8B (Anno)	<b>0.866</b>	0.849	<b>0.906</b>	<b>0.815</b>	<b>0.874</b>	<b>0.938</b>	<b>0.809</b>	<b>0.918</b>
TextPecker-8B (Anno + Syn)	<b>0.901</b>	0.917	<b>0.955</b>	<b>0.995</b>	<b>0.850</b>	<b>0.931</b>	<b>0.840</b>	<b>0.944</b>

### E.4. Statistics of the RL Prompt Set for VTR

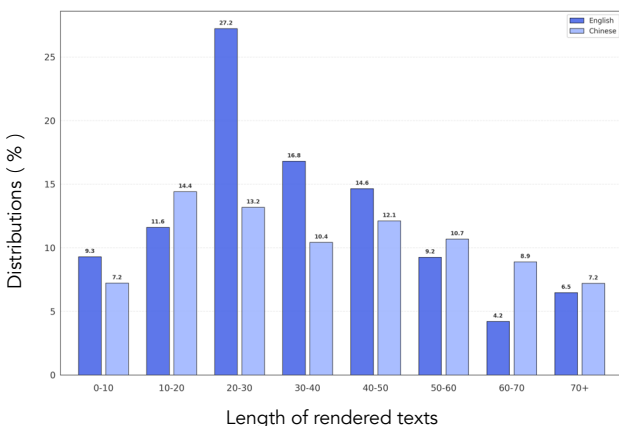


Figure 9. Statistics of the RL prompt set for RL-based VTR optimization (English: word-level; Chinese: character-level).

We present the statistics of the curated prompt set used for RL-based VTR optimization in Fig. 9. The prompt set is designed to encompass diverse text lengths and content for effective reinforcement learning.

For English text rendering, we curate prompts from TextAtlas5M [49], ensuring a rich and varied dataset. For Chinese text rendering, we adopt a similar paradigm as described in the main paper, starting with a comprehensive text corpus sampled from WanJuan1.0 [23], which covers a wide range of modern Chinese common characters. Additionally, we use Qwen3-235B-A22B [60] to generate diverse style descriptions of fonts. These style descriptions are integrated with the corpus to create the final prompt set. The statistics are visualized in Fig. 9.

### E.5. Statistics of the GenTextEval Dataset

To facilitate re-evaluation with TextPecker and build upon the strengths of existing benchmarks, we construct a dataset named GenTextEval, which integrates English and Chinese prompts from multiple sources [6, 14, 20, 49]. In light of the limited availability of Chinese-rendering benchmarks [6, 20, 55] (with ChineseWord remaining unavailable for open-source at the time of our experiments), this dataset is further enriched with Chinese prompts curated as described in Sec. E.4. The final GenTextEval dataset comprises 314 prompts for English rendering and 417 prompts for Chinese rendering. Following the traditional paradigm, each prompt generates four distinct image outputs to ensure fairer assessment. We offer a statistical overview of the GenTextEval dataset in Fig. 10.

### F. Prompt Template for TextPecker

We present the prompting templates used for TextPecker’s training and testing in Fig. 11. To ensure consistency and comparability across evaluations, we adopt the identical template for all other MLLM baselines.

### G. Additional Implementation Details

This section provides further implementation details, supplementing the overview in the main paper. We employ the Flow-GRPO [34] framework for all Reinforcement Learning (RL) based VTR optimization experiments. Notably, Flow-GRPO is an actively evolving repository, and the implementations reported here reflect the stable version available at the time of our experiments. As noted in the main paper, the overall methodology adheres to Flow-GRPO’s core design, while the specific hyperparameters are carefully tuned for each base model (building upon the framework’s default configurations) to ensure stable and effective training. The resolution for all generated images is set to  $512 \times 512$  pixels. The model-specific configurations are detailed below.

**SD3.5-M [16]:** We use 30 sampling steps for training and

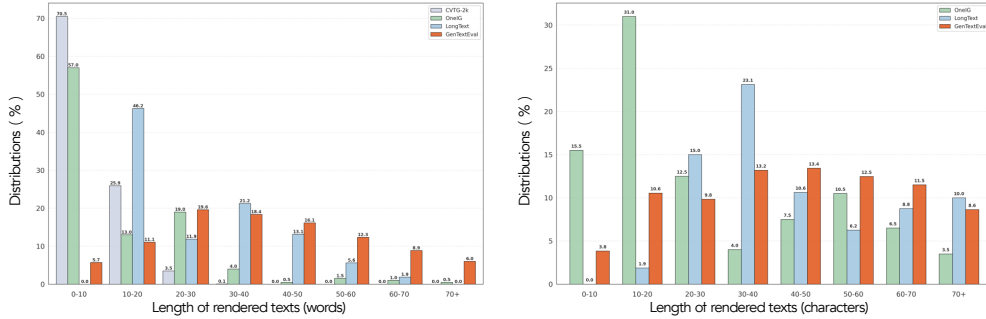


Figure 10. Comparison among CVTG-2K[14], OneIG-Bench[6], LongText-Bench[20], and Our Proposed GenTextEval-Bench with Respect to the Length of Rendered Texts in English (Left) and Chinese (Right).

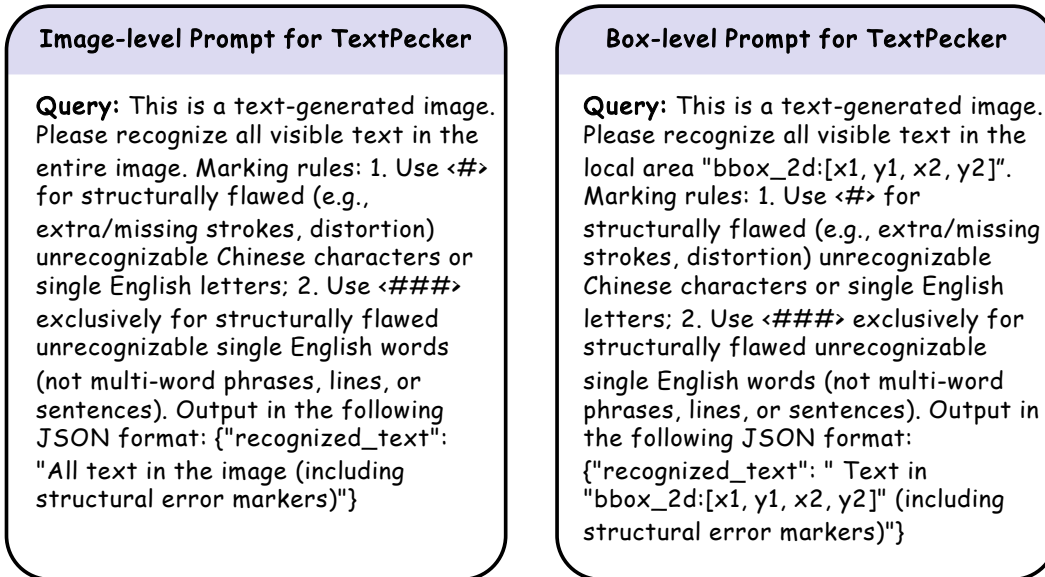


Figure 11. The prompting template used for our TextPecker.

40 for evaluation. The noise level is set to 0.8, and the guidance scale is 1.0 (following the Flow-GRPO-Fast framework, CPS sampling and No-CFG are adopted to improve training efficiency). The KL ratio  $\beta$  is 0.04. For LoRA, we adopt a rank  $r$  of 32 and an alpha  $\alpha$  of 64. Training is conducted using the Flow-GRPO-Fast framework.

**Flux.1[dev] [28]:** We set 14 sampling steps for training and 28 for evaluation. The noise level is 0.9, the guidance scale is 3.5, and the KL ratio  $\beta$  remains 0.04. For LoRA, we use a rank  $r$  of 64 and an alpha  $\alpha$  of 128. No Flow-GRPO variant is employed for this model.

**Qwen-Image [55]:** We employ 10 sampling steps for training and 50 for evaluation. The noise level is set to 1.2, with a guidance scale of 4.0 and a KL ratio  $\beta$  of 0.004. For LoRA, we adopt a rank  $r$  of 64 and an alpha  $\alpha$  of 128. Training is conducted using the Flow-GRPO-Fast framework.

### G.1. Computational cost and latency.

The evaluator is used only during RL training and run as a separate asynchronous service, hence it adds negligible overhead and does not affect inference latency; on SD3.5-M[16], 100 RL steps take 5.52 h (TextPecker) vs. 5.40 h (PPOCRv5[15]).

### H. Additional Implementation Details on Sec. D

As mentioned in Sec. D, we conducted additional experiments utilizing an enhanced RL baseline. This baseline incorporates several advanced techniques including Flow-GRPO-Fast [30], GRPO-Guard [50], Velocity KL loss, and multi-reward regularization. This section provides the specific hyperparameter details for experiments in Tab. 8 and Tab. 9. LoRA configurations remain identical to those described in Sec. D.

**SD3.5-M [16]:** We use 40 sampling steps for both training

and evaluation. An SDE window of size 12 is applied during the first half of the sampling process. The key hyperparameters are set as follows: a noise level of 0.9, a guidance scale of 4.5, and a learning rate of  $10^{-4}$ . The ratio  $\beta$  for the Velocity KL loss is set to  $10^{-4}$ , and the clipping range is set to  $2 \times 10^{-6}$ .

**Flux.1[dev] [28]:** We set the number of sampling steps to 28 for both training and evaluation. An SDE window of size 9 is used in the first half of the sampling steps. The noise level is 0.9, the guidance scale is 3.5, and the learning rate is  $10^{-4}$ . The Velocity KL loss ratio  $\beta$  is configured to  $10^{-4}$ , and the clipping range is set to  $2 \times 10^{-6}$ .

**Qwen-Image [55]:** We employ 20 sampling steps for training and 50 for evaluation. During training, an SDE window of size 5 is applied to the initial half of the sampling steps. The noise level is set to 1.2, the guidance scale is 4, and the learning rate is  $10^{-4}$ . The Velocity KL ratio  $\beta$  is  $10^{-3}$ , and the clipping range is set to  $2 \times 10^{-5}$ .

## I. Limitations

TextPecker paves a novel path for addressing the core bottleneck in VTR evaluation and RL-based optimization, leveraging a structural-anomaly-aware RL reward that delivers complementary signals for semantic alignment and structural quality. While providing a foundational step towards structurally faithful VTR, our work still has several limitations that point to meaningful directions to be explored.

*First*, our structural anomaly synthesis is contingent upon the availability of stroke-level font data. This dependency currently restricts its application to standard fonts, precluding the generation of anomalies in artistic or proprietary typefaces lacking such data.

*Second*, our work is currently confined to Chinese and English text rendering, with efficient multilingual extension as a key area for future exploration.

*Third*, our TextPecker evaluator is equipped with box-level perception ability, which theoretically enables it to support downstream VTR-related tasks such as text translation and local text editing, which are often challenging for general editing methods [10, 28, 46, 47, 68]. Validating the effectiveness of evaluation and RL optimization on these downstream tasks is left for future work.

*Fourth*, challenges arise in handling artistic text generation (see Fig. 6 above), which is an increasingly demanded scenario. Artistic text often involves deliberate modifications to standard structures, such as connected strokes, added symbols, or pictorial variations, making it inherently difficult to define a single standard or ground truth. Furthermore, artistic designs are continuously evolving, presenting a moving target that conflicts with the structural consistency objectives of our current framework. Addressing the evaluation and optimization of artistic text generation remains a challenging

yet impactful research direction, necessitating the integration of creative expression with principles of structure-aware textual modeling.

Table 14. Key parameters for canonical text rendering and structural anomaly construction.

Parameter Category	Canonical Chinese Text	Canonical English Text	Structural Anomaly Construction
<b>Basic Text Configuration</b>			
Vertical text probability	10%	10%	10%
Number of elements per sample	3–10	3–10	3–10
Text length range	1–25 characters	3–25 characters	1–25 characters
<b>Font Settings</b>			
Number of font types	976	976	976
Font size range	50–100 pt	50–100 pt	50–100 pt
<b>Layout Parameters</b>			
Horizontal spacing between elements	50–200 px	50–200 px	50–200 px
Vertical line spacing	10–20 px	10–20 px	10–20 px
Length ratio range	0.8–1.0	0.8–1.0	0.8–1.0
Random offset probability	20%	20%	20%
Random offset range	10–30 px	10–30 px	10–30 px
Image margin	15 px	15 px	15 px
Flow layout probability	80%	80%	80%
Curve layout probability	20%	20%	20%
<b>Style Effects</b>			
Style application probability	25%	25%	25%
- Text border (probability)	100%	100%	100%
Size ratio	5–15%	5–15%	5–15%
Alpha	1.0	1.0	1.0
- Text shadow (probability)	0%	0%	0%
- Text extrusion (probability)	0%	0%	0%
<b>Geometric Transformation</b>			
Transformation application probability	50%	50%	50%
- Perspective x (weight)	1	1	1
Percents	0.8	0.8	0.8
- Perspective y (weight)	1	1	1
Percents	0.8–1	0.8–1	0.8–1
- Trapezoidate x (weight)	1	1	1
Percent	0.8–1	0.8–1	0.8–1
- Trapezoidate y (weight)	1	1	1
Percent	0.8–1	0.8–1	0.8–1
- Skew x (weight)	2	2	2
Angle	0–30°	0–30°	0–30°
- Skew y (weight)	2	2	2
Angle	0–10°	0–10°	0–10°
- Rotate (weight)	3	3	3
Angle	0–10°	0–10°	0–10°
<b>Structural Anomaly Generation</b>			
Anomaly generation probability	0%	0%	50%
- Deletion (probability)	–	–	40%
- Insertion (probability)	–	–	40%
- Swapping (probability)	–	–	40%





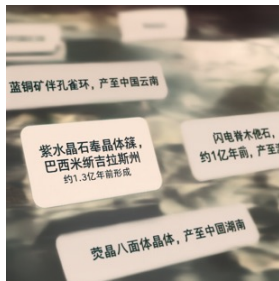
"prompt": "一幅充满奇思妙想的漫画风格插图，描绘两位办公室员工在公园长椅上共进午餐时的幽默互动。对话框自然地按照对话流程排列。画面左上角，第一位员工的对话框内容为：“我带了一份新鲜沙拉，开始健康生活！”右上角第二位员工的对话框位置，其略显怀疑的表情下写着：“早上会议时你不是在吃甜甜圈吗？”左下角第一位员工防御性地回应：“平衡是关键！绿叶蔬菜可以抵消甜甜圈的糖分。”右下角第二位员工带着笑意和调侃的语气说：“啊，我搞错了。你应该给HR发邮件，建议推出新的甜甜圈沙拉健康计划。”诙谐的面部表情伴随着机智的对话，对话框以对角线排列方式自然引导观者体验这场幽默互动。；  
 "target": "我带了一份新鲜沙拉，开始健康生活！早上会议时你不是在吃甜甜圈吗？平衡是关键！绿叶蔬菜可以抵消甜甜圈的糖分。啊，我搞错了。你应该给HR发邮件，建议推出新的甜甜圈沙拉健康计划。；  
 "pecker\_qua": 0.8888888888888888,  
 "pecker\_sem": 0.5802469135802469,  
 "recognized\_text": "早上会议时你不是在 我带了一份新鲜沙拉 吃甜甜圈吗 开始健康生活 啊 我搞错了 你<#><#>HR 平衡是关键 绿叶蔬菜可以抵消甜甜圈的糖分 <#><#><#><#><#>"



"prompt": "阳光明媚的一天，繁忙的游乐园入口处挂满了五彩缤纷的横幅，入口上方悬挂着一条醒目的横幅，用清晰粗体的字母写着：“欢迎来到冒险王国，乐趣永无止境！”在问候语下方，稍小一些的文字写着：“体验惊险刺激的游乐设施，美味可口的美食和难忘的家庭时光。售票处附近的小型横幅用易读的文字标明：“工作日折扣：12岁以下儿童五折！”以及“年卡持有者专属通道”。其他附近标识牌显示着“园区每日上午10点至晚上9点开放”等信息。游客们稍作停留，阅读这些引人注目且充满吸引力的文字信息后，兴奋地朝公园入口走去。；  
 "target": "欢迎来到冒险王国，乐趣永无止境！ 体验惊险刺激的游乐设施、美味可口的美食和难忘的家庭时光 工作日折扣：12岁以下儿童五折！ 年卡持有者专属通道 园区每日上午10点至晚上9点开放，  
 "pecker\_qua": 0.9864864864864865,  
 "pecker\_sem": 0.8227848101265822,  
 "recognized\_text": "欢迎来到冒险王国 乐趣永无止境 体验惊险刺激的游乐设施、美味可口的美食和难忘的家庭时光 工作日折扣：12岁以<#>儿童五折 <#>卡每日上午10点至 <#>晚上9属通道"



"prompt": "A humorous cartoon-style comic panel set inside an art museum, depicting a confused visitor engaging in playful dialogue with the enthusiastic tour guide about an abstract painting. Speech bubbles are positioned naturally to guide viewers easily through their conversation. At the upper-left, the puzzled visitor's speech bubble reads, "Are you sure this upside-down struggle means deep meaning and pizza cravings?" In the top-right corner, the smiling guide replies confidently, "Precisely! Humanity often struggles between deep meaning and pizza cravings." Lower-left corner speech bubble shows the visitor responding thoughtfully, "Well, in that case, I deeply resonate with this masterpiece." Finally, bottom-right side next to the guide, a cheerful bubble summarizes, "Excellent! True art speaks clearly to those who hunger for understanding!". The humorous expressions and clear diagonal speech bubble arrangement naturally guide viewers through the amusing exchange from top-left to bottom-right".  
 "target": "Are you sure this upside-down triangle represents humanity's struggle? Precisely! Humanity often struggles between deep meaning and pizza cravings Well, in that case, I deeply resonate with this masterpiece Excellent! True art speaks clearly to those who hunger for understanding",  
 "pecker\_qua": 0.591596638654622,  
 "pecker\_sem": 0.4777591036414566,  
 "recognized\_text": "THE YOU OFF ARE WRAMGUS STRUGGLE, SUEE THIS THEYAI IE PESINOUT UPSIDE-DOWN HUMANITY,G<#><#>ides. STRVGGLS DEEP MEANING AND PIZZA CRAVINGS? WELL, IN THAT CASE, I DEEPLY REMOTANTE WITH THIS MASTERPIECES EXPELLENT! \TRUE ART CLEARLY NEXTES TO THOSE WHO HUNGER FOR UNDERSTANDING"



"prompt": "一个精心陈列的矿物和晶体标本的玻璃展柜。每个标本都配有详细且易于阅读的信息标签；其中一个显眼的标签清晰标注着“紫水晶石英晶簇，巴西米纳斯吉拉斯州”，下方附有更小字号的说明文字明确写着“约1.3亿年前形成”。附近的其他信息标签精准标注着诸如“蓝铜矿伴孔雀石，产自中国云南”、“闪电脊木化石，约1亿年前，产自澳洲”以及“萤石八面体晶体，产自中国湖南”等展品信息。这些印刷整齐、简洁明了的标签有效吸引并教育着观众，增强他们在欣赏展示矿物标本时的互动体验与理解深度。；  
 "target": "紫水晶石英晶簇，巴西米纳斯吉拉斯州 约1.3亿年前形成 蓝铜矿伴孔雀石，产自中国云南 闪电脊木化石，约1亿年前，产自澳洲 萤石八面体晶体，产自中国湖南，  
 "pecker\_qua": 0.9333333333333333,  
 "pecker\_sem": 0.44285714285714284,  
 "recognized\_text": "蓝铜矿伴孔雀石 产于中国云南 闪电脊木 <#> 紫水晶石英晶簇 约1亿年<#> 产于<#> 巴西<#> 吉拉斯州 约1.3亿年前形成 荧晶八面体晶体 产于<#> 湖南"



"prompt": "A lively, crowded outdoor marketplace fills a sunny plaza, bustling energetically with shoppers weaving among vibrant vendor stands overflowing with fresh, colorful goods. Drawing clear attention at the heart of this dynamic market scene is a large, rustic wooden sign prominently hung above a popular stall, displaying attractive, easily readable lettering that warmly announces "Farm Fresh & Locally Produce". Beneath this main headline, elegant yet simple text proclaims encouraging messages, clearly stating "Taste Nature's Best Support Local Farmers!" and the enticing incentive "Special Offer: Organic 10% Off Today Only!". Scattered artfully around the stall are smaller, charmingly handwritten chalkboard-style signs clearly displaying inviting additional notes such as "Fresh Apples, Strawberries and Seasonal Veggies Available" further engaging and drawing in curious visitors. Shoppers frequently pause to thoughtfully read and appreciate these inviting, vividly presented signs, adding warmth and authenticity to the overall bustling marketplace atmosphere".  
 "target": "Farm Fresh & Locally Produce Taste Natures Best Support Local Farmers! Special Offer: Organic 10% Off Today Only! Fresh Apples, Strawberries and Seasonal Veggies Available",  
 "pecker\_qua": 1.0,  
 "pecker\_sem": 0.71,  
 "recognized\_text": "Farm Fresh & Locally Produce. Taste Nature's Best Support Local Farmers! Special Offer: Organic 10% Off Today Only!"

Figure 13. This figure presents evaluation samples of TextPecker, showcasing its performance in detecting structural anomalies across diverse text rendering scenarios.  $\omega = 1$  for structural quality score visualization.